Science of the Total Environment 924 (2024) 171571

Contents lists available at ScienceDirect

Science of the Total Environment

journal homepage: www.elsevier.com/locate/scitotenv

Predicting natural arsenic enrichment in peat-bearing, alluvial and coastal depositional systems: A generalized model based on sequence stratigraphy

Alessandro Amorosi [a,*], Irene Sammartino [b]

[a] Department of Biological, Geological and Environmental Sciences (BiGeA), University of Bologna, Via Zamboni 67, 40126 Bologna, Italy
[b] National Research Council (CNR), Institute of Marine Science (ISMAR), Via Gobetti 101, 40129 Bologna, Italy

HIGHLIGHTS

- The subsurface of the Po Plain is severely impacted by natural As contamination.
- Background levels in solid matrices vary as a function of depositional environment.
- Total As from peat-bearing deposits exceeds threshold values for contaminated soils.
- We delineate the highest As-hazard zones beneath modern deltas and coastal lowlands.
- Sequence stratigraphic models may help predict subsurface As distribution worldwide.

GRAPHICAL ABSTRACT

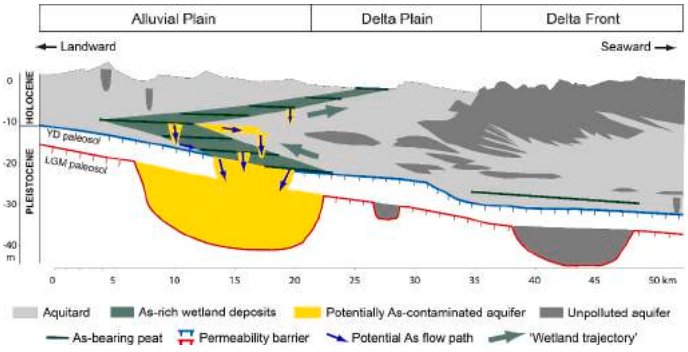

ARTICLE INFO

Editor: Christopher Rensing

Keywords:
Contamination
Aquifer
Delta
Geochemistry
Po Plain
Quaternary

ABSTRACT

Hazardously high concentrations of arsenic exceeding the threshold limits for soils and drinking waters have been widely reported from Quaternary sedimentary successions and shallow aquifers of alluvial and coastal lowlands worldwide, raising public health concerns due to potential human exposure to arsenic. A combined sedimentological and geochemical analysis of subsurface deposits, 2.5–50 m deep, from the SE Po Plain (Italy) documents a systematic tendency for naturally-occurring arsenic to accumulate in peat-rich layers, with concentrations invariably greater than maximum permissible levels.

A total of 366 bulk sediment samples from 40 cores that penetrated peat-bearing deposits were analysed by X-ray fluorescence. Arsenic concentrations associated with 7 peat-free lithofacies associations (fluvial-channel, levee/crevasse, floodplain, swamp, lagoon/bay, beach-barrier, and offshore/prodelta) exhibit background values invariably below threshold levels (<20 mg/kg). In contrast, total arsenic contents from peaty clay and peat showed 2–6 times larger As accumulation. A total of 204 near-surface (0–2.5 m) samples from modern alluvial and coastal depositional environments exhibit the same trends as their deeper counterparts, total arsenic peaking at peat horizons above the threshold values for contaminated soils.

The arsenic-bearing, peat-rich Quaternary successions of the Po Plain accumulated under persisting reducing conditions in wetlands of backstepping estuarine and prograding deltaic depositional environments during the Early-Middle Holocene sea-level rise and subsequent stillstand. Contamination of the Holocene and underlying Pleistocene aquifer systems likely occurred through the release of As by microbially-mediated reductive

* Corresponding author.
E-mail addresses: alessandro.amorosi@unibo.it (A. Amorosi), irene.sammartino@bo.ismar.cnr.it (I. Sammartino).

https://doi.org/10.1016/j.scitotenv.2024.171571
Received 31 December 2023; Received in revised form 23 February 2024; Accepted 6 March 2024
Available online 16 March 2024

dissolution. Using high-resolution sequence-stratigraphic concepts, we document that the Late Pleistocene-Holocene lithofacies architecture dictates the subsurface distribution of As. The "wetland trajectory", i.e. the path taken by the landward/seaward shift of peat-rich depositional environments during the Holocene, may help predict spatial patterns of natural As distribution, delineating the highest As-hazard zones and providing a realistic view of aquifer contamination even in unknown areas.

1. Introduction

Arsenic is a natural component of the Earth's crust that is widely distributed in the environment. Arsenic is a known carcinogen and long-term exposure through drinking water and food have raised public health concerns due to chronic arsenic poisoning. Groundwater and surface water contamination by arsenic of natural origin affects >140 million people in at least 70 countries worldwide (Ravenscroft et al., 2009; Wang et al., 2019). Tens of millions of people in south and southeast Asia routinely consume groundwater that has unsafe arsenic levels (Polizzotto et al., 2008).

Arsenic has multiple natural sources and geochemistry of parent rocks is one of the major factors that govern As distribution in the environment (Zuzolo et al., 2020). Specific geologic conditions that might account for high As concentrations in arsenic-affected river basins are areas of sulphide mineralisation (Chen et al., 2024), where mineral dissolution can be enhanced by mining activity (Sarti et al., 2020). Around mining sites, the primary source of As in groundwater is predominantly natural and mobilized through complex biogeochemical interactions within various aquifer solids and water. High-arsenic groundwaters can also be associated with geothermal sources (hot springs). In these regions, sulphide minerals such as arsenopyrite and As-substituted pyrite, are susceptible to oxidation in the near-surface environment and release significant quantities of As in the sediments (Herath et al., 2016). Metamorphic, felsic volcanic (ignimbrite, lava and tuff) and plutonic parent rocks with an abundance of As-bearing minerals represent additional potential sources for As.

Away from these natural sources of contamination, hazardously high As concentrations exceeding the regulatory limits for drinking waters have been repeatedly recorded in Quaternary alluvial aquifers, in association with abundant organic matter (Smedley and Kinniburgh, 2002; González et al., 2006; Wang et al., 2019). The majority of the recognised high-As groundwater provinces are in Holocene unconsolidated sediments associated with peat-bearing deposits of large deltaic plains, such as low-lying areas of the Bengal Basin (Chatterjee et al., 1995; Bhattacharya et al., 1997; Acharyya et al., 2000; Acharyya and Shah, 2007; Weinman et al., 2008; Desbarats et al., 2014; Ghosh and Donselaar, 2023), the Ganges Delta (van Geen et al., 2003; Mukherjee et al., 2011; Chakraborty et al., 2020), the Red River Delta (Berg et al., 2001, 2008; Winkel et al., 2011; Postma et al., 2012, 2016; Stahl et al., 2016; Dang et al., 2020; Kazmierczak et al., 2022), and the Mekong Delta (Polya et al., 2005; Berg et al., 2007; Papacostas et al., 2008; Stuckey et al., 2015; Huyen et al., 2019).

Recent studies have related arsenic contamination to fluvial geomorphology (Donselaar et al., 2017; Das and Mondal, 2021; Ghosh et al., 2021; Kumar et al., 2021; Paszkowski et al., 2021; Kazmierczak et al., 2022; de Meyer et al., 2023), focusing on arsenic poisoning in groundwater of very shallow, juxtaposed sandy point-bar aquifers and clay plugs formed in adjacent oxbow-lakes (Donselaar et al., 2017; Ghosh and Donselaar, 2023). In these near-surface studies, however, the role of stratigraphic architecture in As concentration has received relatively little attention, and the vertical stacking of distinct lithofacies associations has hardly been incorporated in models for As-hazard simulations, with few notable exceptions from the West Bengal (McArthur et al., 2004, 2008, 2011; Hoque et al., 2012).

In the Bengal Basin, accurate sedimentological data (Weinman et al., 2008) and the lithostratigraphic architecture of the subsurface hydrogeological system (Goodbred and Kuehl, 2000; Goodbred et al., 2014) have been integrated in the model by hydrostratigraphic data (Winkel et al., 2011; Chakraborty et al., 2022b). Aquifer/aquitard relations (Mukherjee et al., 2011), aquifer connectivity and surficial aquitard thickness (Chakraborty et al., 2020) have been investigated as potential controlling factors of groundwater and contaminant flow paths. McArthur et al. (2004, 2008) investigated the petrophysical properties of the aquifer/aquitard system within a high-resolution stratigraphic framework and documented a strong influence of paleosol/channel belt sand bodies on As distribution. For all other deltas, however, a comprehensive model of As distribution is lacking.

The Venetian-Po Plain alluvial/coastal system, in Italy (Fig. 1), is among the most affected European regions by arsenic pollution and several conceptual models have been proposed for interpreting As dynamics in this region (Rotiroti et al., 2021). A survey on As concentration in wheat from Italian agricultural areas documented anomalously high values in the Venetian area (Cubadda et al., 2010) and As concentrations >400 μg/L were reported from groundwater of the Venetian Plain (Carraro et al., 2015). For this region, a possible source for As from felsic volcanic rocks cropping out in the Alpine Brenta River catchment was suggested by elevated (44 mg/kg) average As concentrations observed in alluvial sediments (Ungaro et al., 2008).

In the Po Plain, south of Po River (Fig. 1), far from hydrothermal, volcanic or metamorphic sources, environmentally critical As concentrations, greater than the Italian regulatory limit for As in drinking water (10 μg/L - Legislative Decree 152, 2006), have been detected within the late Quaternary, shallow alluvial aquifer (Carraro et al., 2015; Molinari et al., 2015; Filippini et al., 2021; Zanotti et al., 2022). Despite As levels in soils of the Po Plain are invariably lower than the threshold value of 20 mg/kg for uncontaminated soils (Marchi and Ungaro, 2019), As levels in groundwater of the SE Po Plain (Ferrara area) typically range between 21 μg/L and 62 μg/L (Filippini et al., 2021). The highest As levels have been found to be consistent with the occurrence of localized high natural As content associated with vegetal matter (Carraro et al., 2015; Molinari et al., 2015; Filippini et al., 2021). Anomalously high As values have been reported from peat-rich soils of the Po Plain by Di Giuseppe et al. (2014), who raised specific concerns regarding the mobility of this element and its tendency to be taken up by plants.

As for 80 % of the cases of As contamination in alluvial aquifers, where organic matter rapidly accumulates in humid environments (Ravenscroft, 2007), the existing conceptual model for As mobilization in the Po Plain invokes reductive desorption of As or reductive dissolution of iron oxy-hydroxides (Desbarats et al., 2014; Carraro et al., 2015; Molinari et al., 2015; Filippini et al., 2021; Rotiroti et al., 2021). Degradation of peat-derived organic matter under reducing conditions has been inferred to be the driver of As release to groundwater in the Po Plain (Carraro et al., 2015; Rotiroti et al., 2021). Under oxic conditions, As can be mobilized by dissolution of pyrite or by desorption from iron oxides due to an increase in pH (Smedley and Kinniburgh, 2002).

The subsurface stratigraphy of the Po Plain has received huge attention over the last decades and high-resolution sequence stratigraphic studies have led to refined models of facies architecture (Amorosi et al., 2017a, 2019; Bruno et al., 2017; Campo et al., 2020), with particular attention paid to peat-bearing deposits (Bruno et al., 2019; Amorosi et al., 2021a). The Late Pleistocene-Holocene succession of the Po Plain, thus, may serve as a valuable archive for deciphering the role of stratigraphic architecture on natural As distribution.

By examining spatial variations in arsenic levels within the Late Pleistocene-Holocene aquifer system of the SE Po Plain, between Ferrara

and the Po Delta (Fig. 1), using an integrated sedimentological, stratigraphic and geochemical approach, this study examines the role of lithofacies architecture in the subsurface distribution of this potentially hazardous geogenic contaminant. For the sedimentological and stratigraphic characterization of late Quaternary deposits in the investigated area, we used previously published studies about near-surface (Amorosi and Sammartino, 2007) and subsurface geology (Amorosi et al., 2017a, 2017b). The dataset includes mostly unpublished geochemical analyses from a total of 570 bulk samples.

Specific objectives of this study are to: i) delineate a comprehensive framework of background arsenic concentrations in nine different types of solid matrices (lithofacies associations) that reflect sedimentation in distinct depositional environments, ii) compare near-surface (soil) and subsurface distribution of As, iii) elucidate generalized patterns of As concentration as a function of reservoir geometries, and iv) build a predictive model of potential aquifer contamination for modern coastal lowlands worldwide.

2. Methods

In order to compare the near-surface and subsurface datasets, we grouped all samples (570 in total) into the same set of nine lithofacies associations (grouped into five major units in the geological map of Fig. 1). From proximal to distal depositional environments: 63 fluvial-channel sand samples (CH – 12 near-surface + 51 subsurface), 64 crevasse/levee sand and silt samples (CL – 25 + 39), 84 floodplain silt and clay samples (FP – 44 + 40), 64 swamp clay samples (SW – 21 + 43), 49 swamp peaty clay samples (PC – 21 + 28), 40 swamp peat samples (PT – 17 + 23), 43 lagoon/bay clay samples (LA – 12 + 31), 78 beach-barrier sand samples (BB – 36 + 42), and 85 offshore/prodelta clay samples (OF – 16 + 69).

A total of 366 core samples of sediment deposited in pre-industrial times (1000–40,000 years BP) were investigated to evaluate natural (background) concentrations of arsenic in different sedimentary facies. Samples were collected at depths between 2.5 and 50 m, from 40 continuous cores mostly recovered between the Po and Reno rivers (Fig. 1): seventeen 'EM' cores (EM1-EM17), 184S1, 184S3, 184S4, B2, RN1, RN2, RN3, RN4, RN5, RS1, RS2, RS3, RS4, RS5, Casal, 204S8, 205S2, 205S3, 205S5, 205S10, 187S1, 187S3, and Core1. To assist in facies attribution, we used detailed sedimentological analysis from Amorosi et al. (2017a, 2017b) and Bruno et al. (2017, 2019). Stratigraphic correlation and compositional data of the study cores are summarized in Amorosi et al. (2002), Bruno et al. (2017), and Amorosi et al. (2020).

Near-surface samples (204 in total) were collected by hand drilling/shallow coring between 0.1 and 2.5 m depth (Fig. 1). Of these, 128 alluvial (fluvial channel, crevasse/levee, floodplain), swamp and beach-barrier samples come from the coastal plain north of Ravenna (Amorosi and Sammartino, 2007) and from uppermost cores EM (Fig. 1). Ten samples from fluvial point bars and crevasse/levee deposits and 24 samples from freshwater peats and peat-bearing deposits were obtained through shallow coring of the modern Po River channel belt in the central Po Plain and in the Venetian Plain (Bosi, 2019). The dataset also includes unpublished data from coastal swamps of Tuscany (14 samples), the Venice Lagoon (12 samples), and the Adriatic offshore (16 samples) (Fig. 1).

Samples were analysed without sieving, in order to obtain accurate geochemical characterization of individual lithofacies assemblages in terms of their As content. In preparation for chemical analyses, samples were oven dried at 50 °C, powdered and homogenized in an agate mortar. Chemical analyses were carried out by X-ray fluorescence (XRF) analysis at University of Bologna laboratories, using a Panalytical Axios 4000 spectrometer. Geochemical analyses were each held to the same standards for error and reproducibility, allowing for comparable

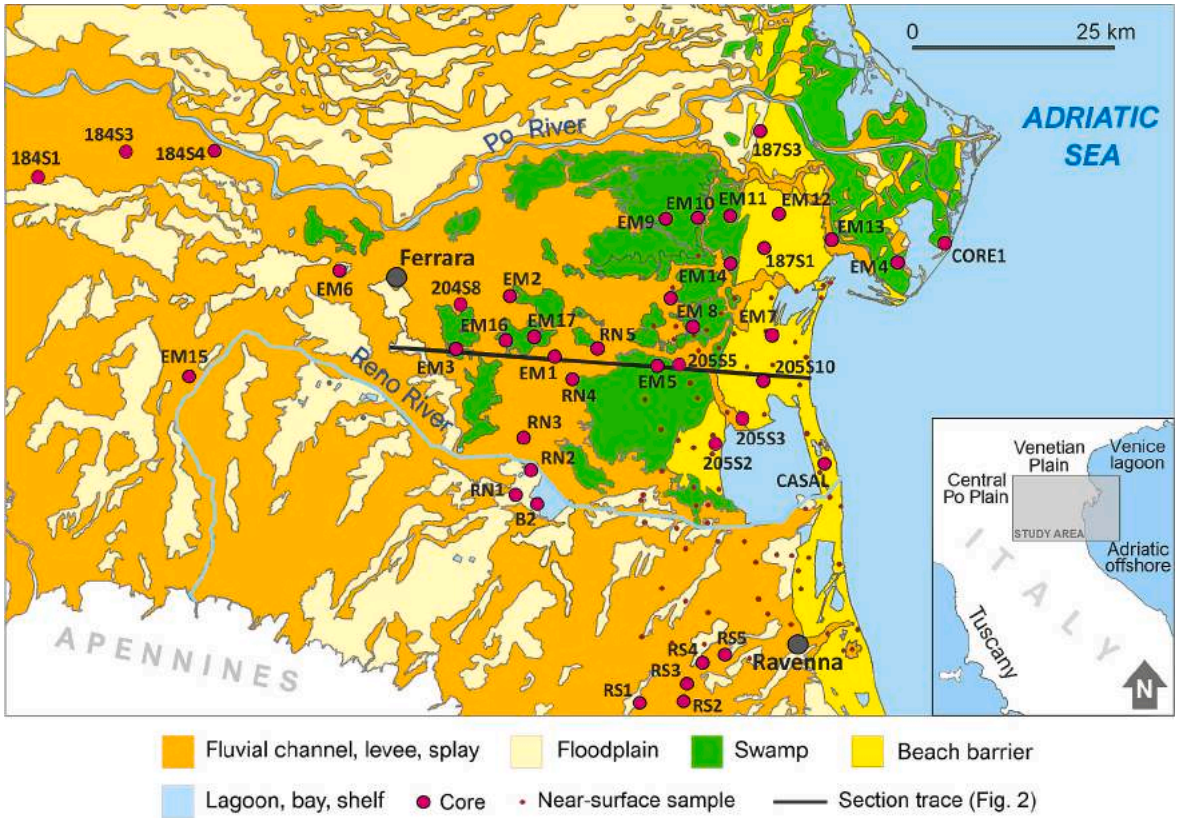

Fig. 1. Geological map of the southeastern Po Plain, with locations of the 40 study cores and hand drillings. Sampling regions around the study area are shown in the inset.

datasets. The matrix correction methods of Franzini et al. (1972), Leoni and Saitta (1976), and Leoni et al. (1982) were followed. The estimated precision and accuracy for trace-element determinations was 5 %. For elements with low concentration (<10 ppm), the accuracy was 10 %. Loss on ignition (LOI) was determined by heating a known amount of sample in a muffle furnace at 750 °C for 1 h after drying at 110 °C in an oven for 24 h. The loss in mass of the sample corresponded to LOI.

3. The Quaternary aquifer system of the Po Plain

3.1. Surficial geology

The Po Plain (Fig. 1) is one of the widest alluvial plains in Europe. It has low relief, with gentle slope from west to east. The Po River, 652 km in length, is the major trunk river and flows from the Western Alps to the Adriatic Sea; it is intersected by a dense network of transverse tributaries from the Alps (in the north) and the Apennines (in the south).

The bulk of the study region consists predominantly of alluvial deposits of Apennine provenance (Fig. 1): fluvial-channel, crevasse and levee sands and silts in lateral transition to floodplain overbank fines (silts and clays). Amalgamated sand bodies attributable to the Po River are present in the Ferrara area, where they form a W-E trending channel belt that roughly coincides with the axis of the present Po River course.

The alluvial plain grades seawards into an intricate coastal plain that includes, SW of the modern Po Delta (east of Ferrara), an abandoned Po Delta lobe that was active up to the XII Century A.D. (Bondesan et al., 1995; Correggiari et al., 2005; Stefani and Vincenzi, 2005) and that hosts a series of marshy swamps (Fig. 1). Lower delta plain subenvironments include bays and lagoons. Coastal deposits consist almost entirely of beach-barrier sand (nearshore to aeolian facies associations) of post-Roman age, elongated parallel to the present shoreline (Fig. 1). These beach-ridge systems correspond, at least in part, to delta front deposits and show contrasting (Po River versus Apennine) source-rock compositions (Amorosi and Sammartino, 2007; Amorosi et al., 2014). Changes in sediment provenance reflect the abandonment of previously active Po Delta distributary channels and their subsequent incorporation into the Apennine fluvial network (Veggiani, 1974).

Bulk-sediment geochemistry has been used to characterize sediment provenance and to distinguish sediment supplied from (i) an ophiolite-bearing province (Western Alps and NW Apennines), (ii) carbonate and felsic rocks (Central and Eastern Alps), and (iii) siliciclastic turbidites (Northern Apennines) (Amorosi et al., 2002, 2014).

3.2. Subsurface geology and sequence stratigraphic framework

The stratigraphic architecture in the subsurface of the Po coastal plain (Fig. 2) consists of two distinct stratigraphic units, of Late Pleistocene and Holocene age, respectively, that reflect the overwhelming control by the late Quaternary sea-level fluctuations (Campo et al., 2016; Amorosi et al., 2017a).

The Late Pleistocene alluvial succession accumulated during the long phase of relative sea-level fall between about 125 and 30 cal kyr BP and the subsequent sea-level lowstand, between about 30 and 25 cal ky BP, which coincides with the Last Glacial Maximum (LGM). In terms of sequence stratigraphy, this unit includes the falling stage systems tract (FSST) and the overlying lowstand systems tract (LST) (Fig. 2). The "LGM paleosol", narrowly constrained between 29 and 24 cal ky BP, is a prominent stratigraphic unconformity of regional significance that records a mixed eustatic and climatic control related to the Marine Isotope Stage (MIS) 3/2 transition and that represents the sequence boundary of the LGM depositional sequence (Amorosi et al., 2017b). This hiatal surface correlates with laterally extensive, lowstand fluvial channel-belt sand bodies supplied by the Po River and its tributaries (Fig. 2). A younger paleosol, formed between 13 and 11.5 cal ky BP during the short-lived Younger Dryas cold event (YD in Fig. 2), caps the alluvial succession and marks the Pleistocene-Holocene boundary. This hiatal surface correlates laterally with a narrower fluvial channel-belt that is commonly amalgamated onto the underlying LGM channel belt (Amorosi et al., 2017b).

The LGM and YD paleosols, 0.5–1.5 m thick, are pedogenically

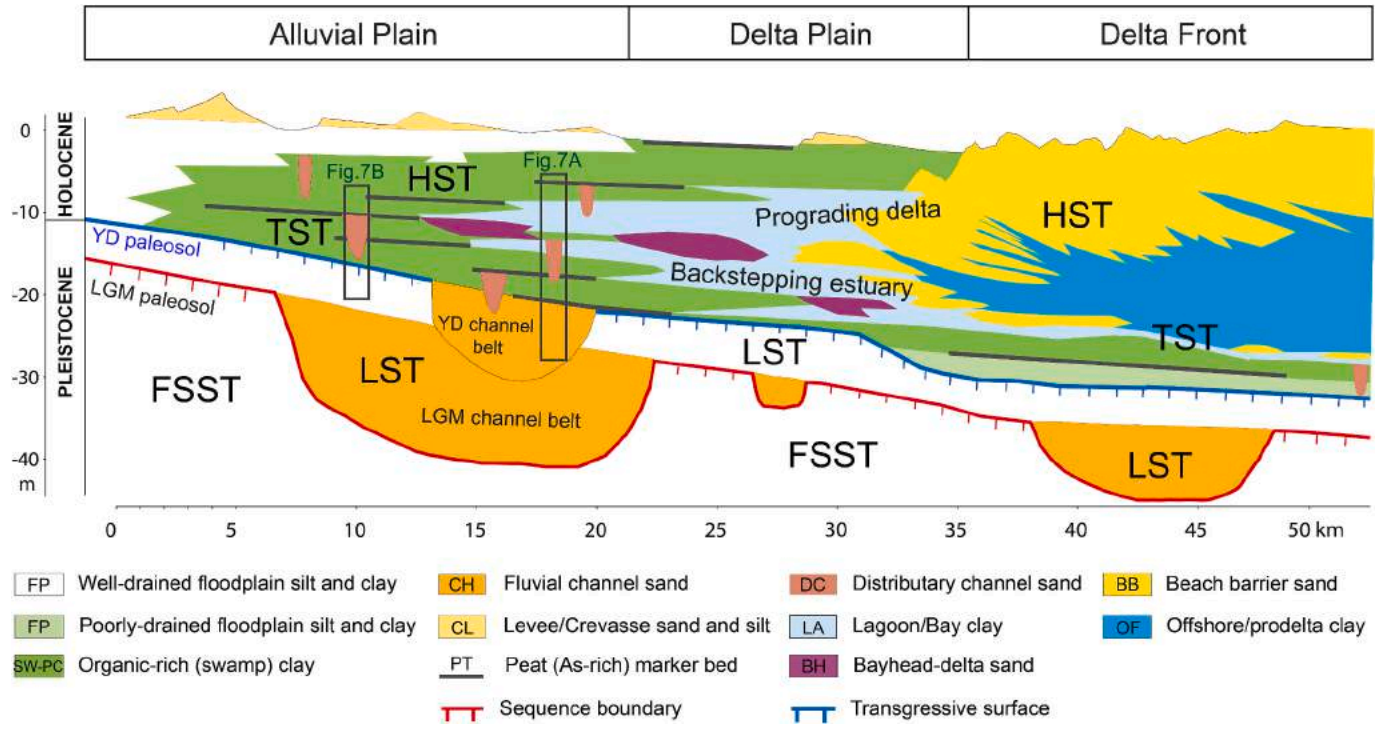

Fig. 2. Lithofacies architecture and sequence-stratigraphic interpretation of Late Pleistocene-Holocene deposits from a coring transect in the SE Po Plain (after Amorosi et al., 2017a, 2017b). FSST: falling-stage systems tract, LST: lowstand systems tract, TST: transgressive systems tract, HST: highstand systems tract. Core intervals of Fig. 7 are indicated.

altered floodplain deposits, developed over time spans of just a few thousand of years and mostly partitioned into A-Bk horizons. The most notable paleosol features are dark, organic-matter-rich and carbonate-free mineral surface horizons (A) that overlie bright calcic horizons (Bk) typified by the accumulation of secondary carbonates in the form of pedogenic nodules. Paleosol profiles exhibit a homogeneous geochemical signature that fingerprints a moderate degree of weathering, with little strike- and dip-oriented variability across the different study localities (Amorosi et al., 2021b).

The "YD paleosol" is overlain by a variety of Holocene facies associations formed in alluvial, freshwater, brackish, coastal and shallow-marine environments (Fig. 2). The Holocene deposits denote a retrogradational/progradational stacking pattern of facies around the maximum flooding surface that delineates the Early Holocene transgressive systems tract (TST) and the overlying highstand systems tract (HST), of Middle-Late Holocene age. The YD paleosol, in particular, marks the transgressive surface (Fig. 2). Millennial-scale depositional packages, a few m thick, have been recognised within the Holocene succession of the Po Plain (Amorosi et al., 2017a). These packages, bounded by flooding surfaces, are stacked rhythmically and represent small-scale parasequences. Laterally continuous peat layers represent key stratigraphic markers that occur at discrete stratigraphic levels (Bruno et al., 2019) and correlate distally with tongues of lagoon deposits (Amorosi et al., 2021a – Fig. 2).

The Quaternary aquifer system of the Po Plain is a multi-layered aquifer system (Filippini et al., 2015; Rotiroti et al., 2017) that reflects a characteristic (Milankovitch-scale) cyclic fluvial architecture, with distinctive cyclic changes in lithofacies and channel stacking patterns (Amorosi et al., 2008). Its upper portion includes a semi-confined Holocene aquifer underlain by a confined Late Pleistocene (glacial) aquifer. At greater depths, largely continuous aquitard layers split the aquifer into aquifer units that are nearly isolated.

4. Results

4.1. Quaternary lithofacies associations

All samples were classified on the basis of their sedimentological characteristics into nine lithofacies associations (Fig. 2), reflecting the whole spectrum of alluvial, paralic, coastal and shallow-marine Holocene depositional environments in the study area (Fig. 3). Sedimentological features of these lithofacies assemblages, the distinction of which is based on subtle paleoecological indicators (mollusks, benthic foraminifers and ostracods), have been illustrated in detail in previous work (Amorosi et al., 2017a; Bruno et al., 2017) and will only briefly summarized here.

Lithofacies association CH consists of medium to coarse sand (Fig. 3). Sand bodies, 1 to 3 m thick, are cross-stratified, with erosional lower boundaries, sharp tops and general fining upwards (FU) of grain size. Wood fragments and fossils are locally encountered. Within Pleistocene deposits, individual sand bodies commonly are vertically stacked into thicker (up to 20 m) sand bodies. This lithofacies association is interpreted to reflect river-dominated deposits, including fluvial-channel, distributary-channel and bay-head delta systems.

Lithofacies association CL consists of a heterolithic succession of medium to fine-grained laminated sand, silt and clay (Fig. 3), organized in 0.2–0.5-m-thick sand bodies with coarsening-upward trends or sand-silt alternations containing roots with fining-upward grain-size successions. This lithofacies association is inferred to represent channel-related deposits, formed in the proximity of fluvial channels or distributary channels in response to crevassing (crevasse splays) or overbank processes (levee deposits), respectively.

Lithofacies association FP consists of variegated silt and clay, with abundant plant debris, Fe-Mn oxides, carbonate nodules and pedogenic features (Fig. 3). Weakly-developed paleosols are commonly intercalated. This lithofacies association is generally barren in fossils or may contain at most a few opercula of freshwater mollusks, and is interpreted as formed in a well-drained floodplain environment.

Lithofacies association SW consists of very soft, light grey (iron-reduced) clay with wood debris (Fig. 3). This lithofacies is homogeneous, structureless to faintly laminated and includes a diagnostic freshwater fauna. It formed in a variety of wetland environments, from inner estuary to upper delta plains and represents a swamp margin subenvironment, with no evidence of subaerial exposure.

Lithofacies association PC is a homogeneous, organic-rich, grey clay with abundant wood debris, such as leaves and twigs. Pedogenic features are lacking. Freshwater fossils typify this facies association, which differs from lithofacies SW by the abundance of undecomposed organic matter and common peat intercalations (Fig. 3). This lithofacies accumulated under anoxic conditions contiguous to lithofacies SW, but in slightly deeper position.

Lithofacies association PT is made up almost entirely of plant material in a good state of preservation, locally interbedded with dark clay horizons (Fig. 3). In particular, it comprises dark-grey to black silt and clay, with yellowish brown to brownish black peat showing typical fibrous consistency. Vegetal remains mainly consist of wood fragments,

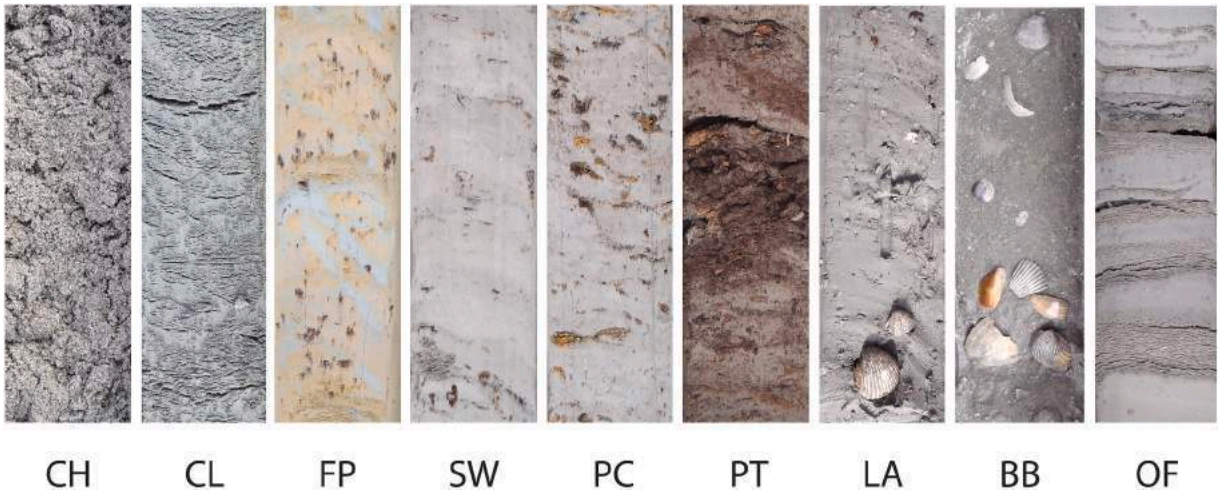

Fig. 3. Representative core photographs of the nine lithofacies associations considered in this work. CH: fluvial channel sand (core EM2), CL: crevasse/levee silty sand (core RN2), FP: floodplain silt and clay (core EM2), SW: swamp clay (core EM4), PC: swamp peaty clay (core EM9), PT: swamp peat (core EM9), LA: lagoon/bay clay (core EM5), BB: beach barrier sand (core EM4), OF: offshore/prodelta sand-clay alternations (core EM13).

roots, stems and leaves. This lithofacies association reflects deposition under waterlogged conditions in standing water, such as the clay-plug fill of the oxbow-lake that surrounds the point bar or a swamp basin in upper delta plain or inner estuary environments of an incised-valley fill.

Lithofacies association LA includes homogeneous grey clay typified by the abundance of a brackish fauna or fossils diagnostic of relatively confined, shallow-marine environments (Fig. 3). Distinct faunal assemblages allow the differentiation of lagoon from bay depositional subenvironments and lower delta plain from outer estuary environments.

Lithofacies association BB consists of well-sorted, fine-medium sand, organized in characteristic coarsening-upward successions, with an abundance of marine fossils (Fig. 3). This lithofacies association is interpreted as formed in beach-barrier environments. The local paucity of fossils has been related to deposition in delta-front environments, close to river mouths.

Lithofacies association OF is made up of bioturbated silty clays with abundant thin sand-silt intercalations (Fig. 3). Fossils are diagnostic of open-marine environments. This lithofacies association is interpreted to reflect a shelf depositional environment. Poorly bioturbated deposits with a typically specialized microfauna indicate prodelta environments, off fluvial mouths.

4.2. Natural arsenic concentrations in peat-bearing deposits exceed regulatory limits

Results of geochemical analyses indicate that arsenic concentrations are significantly different among samples from distinct types of solid matrices (Fig. 4). In particular, all peat-free cored intervals (lithofacies associations CH, CL, FP, SW, LA, BB and OF) have mean As concentrations in the range of 4.6–10.6 mg/kg (Fig. 4A). These values are strikingly consistent with the world baseline concentrations of arsenic in sediments, ranging between 5 and 10 mg/kg, with 7.2 mg/kg as a mean value (Smedley and Kinniburgh, 2002). On the other hand, peat-bearing deposits exhibit elevated arsenic concentrations that typically equal (lithofacies PC) or exceed (lithofacies PT) threshold levels set nationally at 20 mg/kg (Fig. 4A).

Arsenic from lithofacies PT and PC in cored intervals yielded mean concentrations of 28.3 mg/kg and 19.6 mg/kg, respectively (Table 1). These values are two to six times larger than those detected from peat-free deposits. It is remarkable that swamp clay, which is typically intercalated to peaty clay and peat in wetland deposits, but with markedly lower organic matter contents (Fig. 3), had significantly lower As concentrations (8.8 mg/kg), comparable to those of peat-free lithofacies associations.

Consistent with subsurface data, average As contents from near-surface, peat-free deposits (lithofacies associations CH, CL, FP, SW, LA, BB, and OF) yielded almost identical results, with low values in the same approximate range of 4.5–10.5 mg/kg (Fig. 4B). These data are consistent with As contents reported from surficial alluvial deposits of the southern Po Plain (Marchi and Ungaro, 2019) and from lagoonal clays of the modern Po Delta (Zonta et al., 2019). In contrast, organic-rich near-surface samples, such as peat and peaty clay (PT and PC in Fig. 4B), yielded average As concentrations of 26.5 mg/kg and 16.9 mg/kg, respectively (Table 1), 1.5–6 times larger than those detected from peat-free lithofacies associations. Consistent with subsurface deposits, non-organic swamp clay displays lower As contents (10.5 mg/kg) than its peat-bearing counterpart (Fig. 4B).

The comparable levels of As and almost identical patterns of total As distribution in terms of lithofacies associations across both cored intervals and near-surface samples imply that elevated As concentrations are of natural origin and cannot be attributed to contaminant sources. In addition, the content of sediment-bound As is clearly related to sediment grain size, coarser-grained lithofacies associations typically showing lower As levels than finer-grained deposits (Nath et al., 2008; Weinman et al., 2008; Xu et al., 2023). Since small particles have higher surface-area-to-volume ratio than larger grains and a more reactive surface area, elements associated with surface coatings, such as As, are typically most abundant in clay and gradually less concentrated in coarser material (Parks, 1990; Berg et al., 2008). Specifically, background levels of arsenic in sandy lithofacies associations (CH, CL and BB) are narrowly constrained between 4.5 and 7.4 mg/kg, whereas silty and clayey lithofacies associations (FP, SW, LA, and OF) exhibit invariably higher values, between 7.1 and 10.6 mg/kg (Table 1), with almost no overlap.

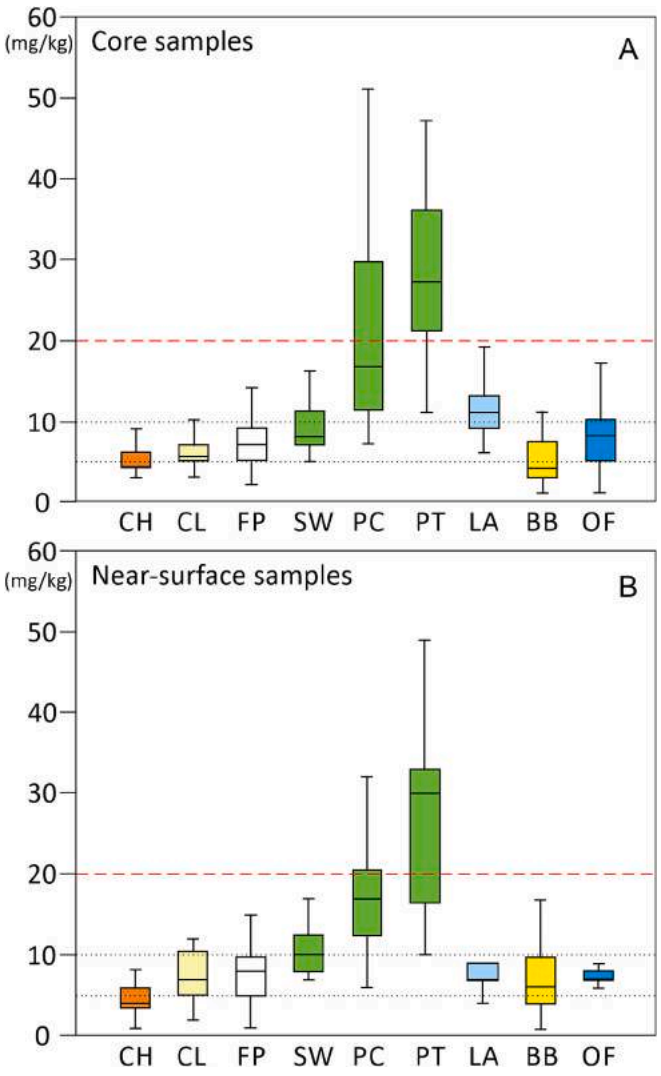

Fig. 4. Summary of background arsenic concentrations from 366 core samples (A) for the nine lithofacies associations investigated in this study, and comparison with As concentrations from 204 near-surface (<2.5 m) samples (B). While As concentrations in most solid phases (CH: fluvial channel, CL: crevasse/levee, FP: floodplain, SW: swamp, LA: lagoon/bay, BB: beach barrier, OF: offshore/prodelta) are in the range of normal concentrations, peat (lithofacies PT) and peat-bearing deposits (lithofacies PC) exhibit As values commonly higher than threshold levels. The lower boundary of box-and-whiskers plots is the 25th percentile, the upper boundary is the 75th percentile, the bold line within the box corresponds to the median, the "whiskers" define minimum and maximum values. The red dashed line indicates the threshold value (20 mg/kg) for uncontaminated lands, according to the Italian regulations. World baseline concentrations of arsenic (dotted lines) are also reported.

Table 1 provides summary statistic data for the nine lithofacies associations analysed in this work. The detailed chemical composition of individual samples from the study area, including the average proportion of As and selected oxides and trace elements in the different lithofacies associations, is shown in Supplementary Table 1.

Table 1
Summary statistics for the nine lithofacies associations examined in this work (mean values are highlighted in grey). Red numbers indicate values above the Italian threshold level (20 mg/kg) for uncontaminated soil.

Core samples	CH	CL	FP	SW	PC	PT	LA	BB	OF
N	47	38	40	41	27	23	29	42	69
Min	3	3	2	5	7	11	6	1	1
Max	9	10	14	16	51	47	19	11	17
Sum	217	223	284	362	528	650	306	214	517
Mean	4.62	5.87	7.10	8.83	19.56	28.26	10.55	5.10	7.49
Std. error	0.20	0.31	0.42	0.40	2.07	1.93	0.54	0.39	0.43
Variance	1.94	3.74	7.22	6.55	115.87	86.11	8.61	6.38	12.55
Stand. dev	1.39	1.93	2.69	2.56	10.76	9.28	2.93	2.53	3.54
Median	4.00	5.50	7.00	8.00	16.00	27.00	10.00	4.00	8.00
25 prcntil	4.00	5.00	5.00	7.00	11.00	21.00	9.00	3.00	5.00
75 prcntil	5.00	7.00	9.00	10.50	28.00	36.00	12.00	7.25	10.00
Skewness	1.39	0.60	0.31	0.87	1.11	0.06	0.96	0.53	−0.22
Kurtosis	2.45	−0.26	−0.16	0.56	1.08	−0.51	1.64	−0.91	−0.40
Geom. mean	4.44	5.57	6.56	8.49	17.07	26.64	10.18	4.48	6.23
Coeff. var	30.14	32.95	37.85	28.98	55.05	32.84	27.81	49.58	47.28

Near-surface samples	CH	CL	FP	SW	PC	PT	LA	BB	OF
N	12	25	44	21	21	17	11	36	14
Min	1	2	1	7	6	10	4	1	5
Max	8	12	15	17	32	49	9	17	9
Sum	54	185	325	221	354	450	80	250	104
Mean	4.50	7.40	7.39	10.52	16.86	26.47	7.27	6.94	7.43
Std. error	0.66	0.66	0.56	0.63	1.24	2.68	0.49	0.75	0.27
Variance	5.18	10.92	14.01	8.36	32.33	122.14	2.62	20.17	1.03
Stand. dev	2.28	3.30	3.74	2.89	5.69	11.05	1.62	4.49	1.02
Median	4.00	7.00	8.00	10.00	17.00	30.00	7.00	6.00	7.00
25 prcntil	3.25	5.00	5.00	8.00	12.50	16.50	7.00	4.00	7.00
75 prcntil	6.00	10.50	9.75	12.50	20.50	33.00	9.00	9.75	8.00
Skewness	0.03	0.05	−0.06	0.88	0.57	0.08	−0.88	0.66	−0.54
Kurtosis	−0.42	−1.18	−0.63	0.02	1.35	−0.41	0.34	−0.44	1.62
Geom. mean	3.79	6.57	6.04	10.18	15.90	23.98	7.08	5.36	7.36
Coeff. var	50.59	44.65	50.67	27.48	33.73	41.75	22.25	64.67	13.68

Our data very well match data from unconsolidated deposits of the Gange Plain (Smedley and Kinniburgh, 2002), where average As concentrations in sands (2.9 mg/kg) are typically lower than in clay (6.5 mg/kg). Arsenic concentrations in sandstones (about 0.5–1.2 mg/kg) are also regularly lower than in shale (13 mg/kg) and coal (up to 24 mg/kg) (Kabata-Pendias and Mukherjee, 2007). Remarkably high total arsenic concentrations, higher than concentrations in "normal" clayey and sandy deposits, have been observed in peats and peaty sediments of the Ganges Delta (Yamazaki et al., 2003).

4.3. Geochemical characteristics of peat-bearing deposits

Organic-rich deposits can be differentiated from their peat-free counterparts by selected geochemical indicators that exhibit strong correlation with arsenic (Fig. 5). Enrichment trends in sulphur (S) with increasing As concentrations occur within lithofacies associations PT and PC, where half of the samples contained S > 8 g/kg (Fig. 5A). On the other hand, peat-free deposits (lithofacies associations CH, CL, FP, SW, LA, BB, and OF) exhibit notably lower S concentrations, almost invariably <8 g/kg (Fig. 5A).

Total iron (Fe_2O_3) reveals a similar lithofacies distribution (Fig. 5B): peat-free deposits have relatively low As concentrations and low (2–7 %) Fe_2O_3 values. In contrast, organic-rich lithofacies are typified by relatively high total iron contents (5–10 %), in association with high As concentrations.

Finally, high As concentrations are generally paralleled by relatively high LOI values (Fig. 5C). Samples from peat-bearing deposits (PT and PC) and peat-free lithofacies associations plot in distinct fields of the LOI/As diagram, with poor overlap. Specifically, LOI is almost invariably lower than 25 % in peat-free deposits, whereas peaty clays and peats commonly have levels in the range of 15–70 %.

Correlation of total As with S, along with generally positive relations between As and Fe_2O_3 and LOI suggest that arsenic is retained in the sediments in the form of sulphide minerals (Molinari et al., 2015), such as arsenopyrite (FeAsS), a chemically stable form under anoxic conditions (Smedley and Kinniburgh, 2002; Yamazaki et al., 2003). Marine waters and peat are naturally enriched in sulphate. In a reducing environment, sulphate binds with Fe, which is present in the organic matter, to form pyrite, with As as co-precipitate (Farooqui and Bajpai, 2003). FeS_2 pyrite can incorporate large amounts (up to ca 10 % wt) of arsenic (Blanchard et al., 2007). Organic-matter-rich wetlands enriched in S, thus can be considered as efficient geochemical traps for As (Langner et al., 2012; Tarvainen et al., 2013; Stuckey et al., 2015; Mikutta and Rothwell, 2016) that can subsequently be released to the groundwater.

5. Discussion

5.1. Stratigraphic control of facies architecture on natural As distribution

The characterization of nine lithofacies associations in terms of background levels of arsenic enables accurate assessment of natural As distribution in the subsurface of the Po Plain. Large differences in arsenic concentration are observed along stratigraphic profiles as a function of peat abundance (Fig. 6): the highest total As values are invariably recorded where peat (PT) and peaty clay (PC) are most abundant, delineating stratigraphic intervals where As-bearing minerals, such as pyrite and iron oxides, are likely to be enriched. Other elements analysed, such as sulphur, reveal broadly similar depth profiles (Fig. 6), supporting the overall correlations with arsenic shown in Fig. 5.

High background concentrations of arsenic in organic-rich deposits suggest that As contamination could be particularly severe in water associated with thick Holocene peat. This hypothesis is fully consistent with data from groundwater of the Holocene aquifer in the Po Plain,

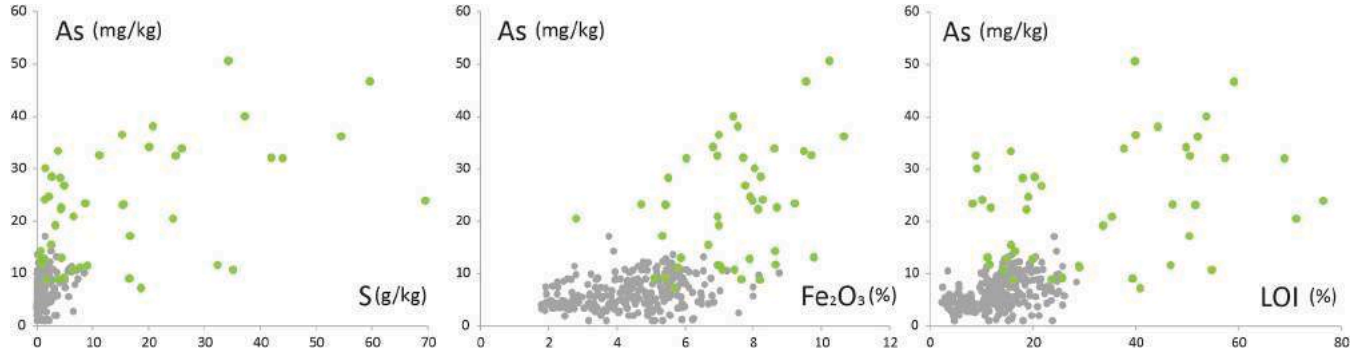

Fig. 5. Scatterplot of As versus S (A), Fe_2O_3 (B) and LOI (C), showing geochemical composition of peats and peat-bearing deposits (in colour) versus non-peaty sediments (in grey). High As concentrations in peat and peaty clay are paralleled by high sulphur and iron values. High LOI indicates an abundance of organic matter. Same dataset as in Fig. 4.

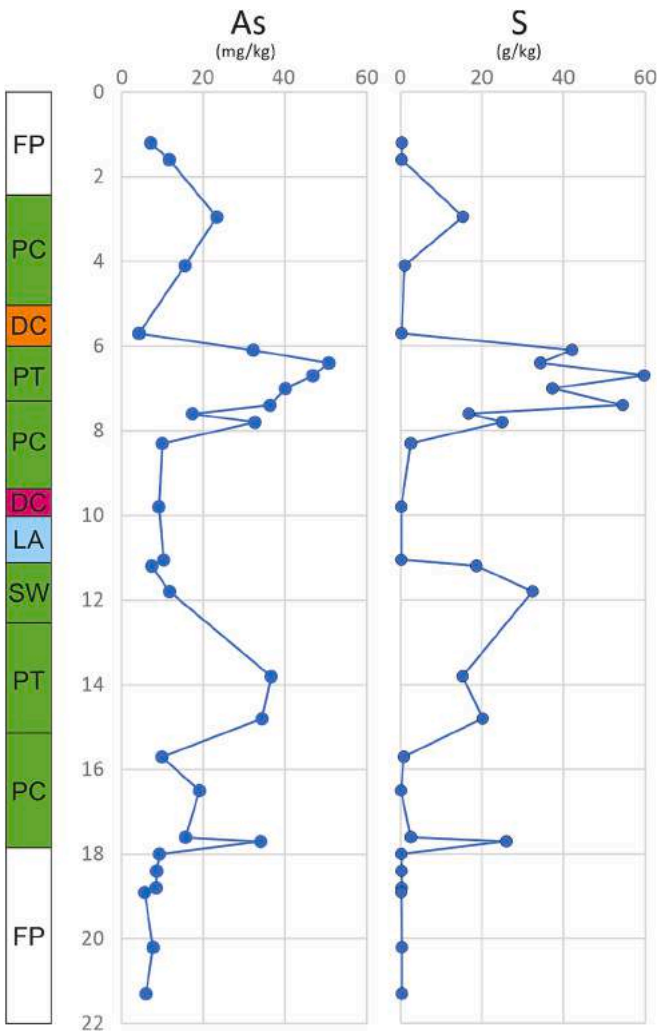

Fig. 6. Depth profiles of total arsenic and sulphur concentrations as a function of lithofacies distribution (data from cores RN4 and RN5 - see Fig. 1, for location). FP: floodplain silt and clay, SW: swamp clay, PC: swamp peaty clay, PT: swamp peat, CH: fluvial-channel sand, CL: crevasse/levee sand and silt, BH: bay-head delta sand, LA: lagoon/bay clay.

where arsenic commonly exceeds the regulatory limits and exhibits background levels three times higher than in regions where peat is scarce or lacking (Filippini et al., 2021).

A sedimentary facies control on groundwater arsenic distribution at the interface between fine-grained, organic-rich deposits and fluvial-channel sand has been documented on a local scale by Papacostas et al. (2008) from the Mekong River delta, where elevated arsenic concentrations arise in regions of recent organic matter deposition. Within scroll bars and abandoned channels, the deposition of rapidly buried reactive organic matter facilitates microbial iron reduction and may trigger arsenic release. The same phenomenon has been described by Donselaar et al. (2017), who observed that compaction of clay-plug sediment may trigger the expulsion of organic-carbon containing pore fluids to the adjacent permeable point-bar sands. The diffusion process of reductive dissolution releases the arsenic from its solid state in the point-bar sands, and the dissolved arsenic can enter the aquifer.

Within the Holocene semi-confined aquifer of the Po Plain, significant As release is expected where organic matter is abundant and vegetal-rich compounds are in contact with paleo-waters (Carraro et al., 2015; Molinari et al., 2015). At these locations, organic-matter-rich deposits may act as a source of As to downgradient aquifers (Fig. 7A). Hydrologic connectivity between confining clays with high As levels and contiguous aquifer-forming sands occurs where thick, Holocene peat-rich successions formed in transgressive estuarine environments cap thick Pleistocene fluvial sand bodies deposited as braided rivers in large paleovalley systems (Fig. 7A). In the study area, estuarine Holocene deposits are made up primarily of organic-matter-rich sediment (lithofacies PT and PC), associated with swamp clay (SW) and highly subordinate meandering distributary-channel (DC) and crevasse/overbank (CL) facies associations (Fig. 7A).

The natural release of As under strongly reducing conditions in the Holocene clay aquitard and its possible downward transport may produce invasion of the Pleistocene sandy aquifer by As and dissolved organic matter, posing severe issues of aquifer contamination to underlying groundwaters (McArthur et al., 2011; Winkel et al., 2011; van Geen et al., 2013; Stuckey et al., 2015). Elevated risks of contamination due to vertical amalgamation of Holocene and Pleistocene fluvial aquifer sands in good vertical hydraulic continuity have been documented from the same area for other peat-related compounds, such as vinyl chloride (Filippini et al., 2016).

5.2. *Predicting subsurface patterns of arsenic concentration using sequence stratigraphy*

Insights gained from well-established sequence-stratigraphic models may help understand the complexities of groundwater paths and provide a basis for building a conceptual model of natural arsenic distribution in the shallow subsurface that might have worldwide application (Fig. 8). As pointed out by previous workers (McArthur et al., 2004, 2011; Weinman et al., 2008; Donselaar et al., 2017), we speculate that stratigraphic architecture of sedimentary facies directly influences spatial patterns of groundwater As distribution within shallow aquifers in a predictable manner, and we develop a conceptual model that predicts potential for occurrence of arsenic in the subsurface of modern coastal lowlands.

The highest concentrations of As are expected within aggradationally stacked, peat-rich deposits (up to 15 m thick) that accumulated around the time of maximum marine ingression (TST/HST boundary in Fig. 2), when eustatic rise decelerated and transgressive estuaries turned into the modern deltas (Stanley and Warne, 1994; Amorosi et al., 2017a). During this period, a high water table and little introduction of clastic material due to retarded river sediment supply made areas landwards of the maximum brackish incursion ideal nucleation sites for widespread, permanent mires (Flint et al., 1995; Jerrett et al., 2011), resulting in thick peat accumulations that in the Po Plain cover the 9–4 cal kyr BP interval of time (Fig. 2).

Areas that have the potential or likelihood of having elevated As concentrations include the innermost, peat-rich portions of estuarine-delta systems buried beneath present-day alluvial plain sediments (Wang et al., 2018 - Figs. 2 and 8). In such regions, arsenic preferentially entrapped in fine-grained, organic-rich sediment of Early-Middle Holocene age (Acharyya et al., 2000) is mobilized by the degradation of organic matter in the upper aquitard, and adjacent Holocene fluvial sediments are sufficiently permeable to allow the passage of soluble organic matter from organic-rich sediments downwards in recharging groundwater (Figs. 7A and 8).

Within the Late Pleistocene-Holocene aquifer system, arsenic will be trapped, accumulating to high concentrations, or diluted in the aquifer flow as a function of: (i) the inherent permeability contrast between the poorly-permeable-clay Holocene sediment and the underlying highly-permeable Late Pleistocene fluvial sand, (ii) the degree of interconnectedness between Holocene and Late Pleistocene fluvial sand bodies, (iii) the more or less heterolithic facies distribution within sandy lithofacies associations (Donselaar et al., 2017) that may cause permeability baffles to fluid flow and compartmentalize the aquifer (Fig. 8). It is important to remark that aquifer recharge efficiency by regional groundwater flux along the palaeovalley axis is high in porous/permeable stacked fluvial sand bodies, and that this process could likely dilute As concentrations,

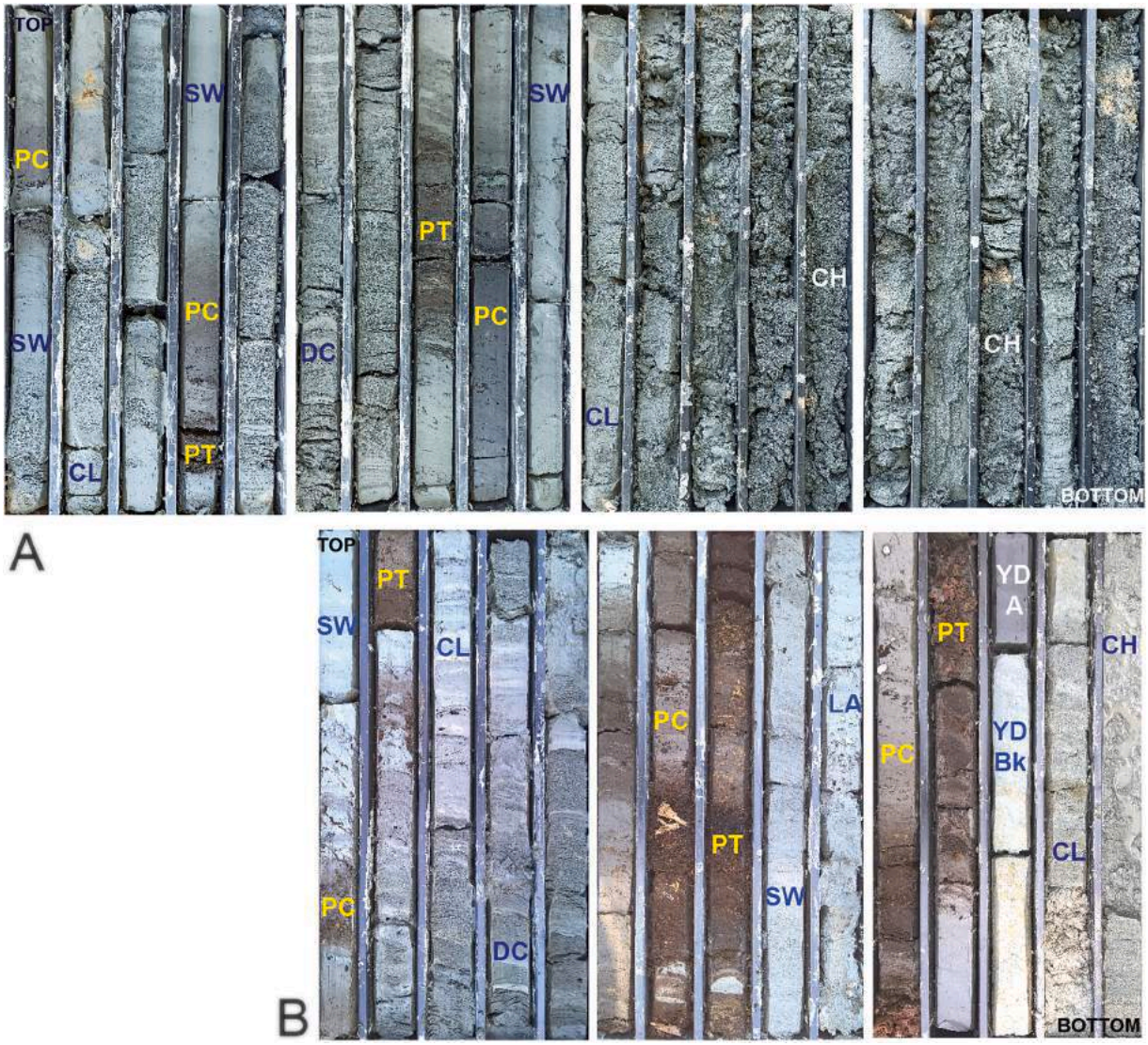

Fig. 7. Discrete layers of As-bearing, estuarine organic-rich lithofacies associations (PT and PC, in yellow) of Early Holocene age associated with swamp (SW), crevasse/levee (CL), lagoon (LA) and distributary channel (DC) deposits overlie Pleistocene fluvial sand (facies CH and CL). See Fig. 2, for approximate stratigraphic position. A (core 184-S4, 5–25 m core depth): the highly permeable fluvial sand below the As-rich peat may represent a conduit for groundwater that is polluted by arsenic and that can migrate downward (and then laterally) to pollute the aquifer. B (core B2, 10–25 m core depth): As-bearing Holocene deposits (lithofacies PT and PC) are separated from underlying Pleistocene fluvial deposits by the stiff Younger Dryas (YD) Inceptisol (see paleosol horizons 'A' and 'Bk'), which acts as a regional permeability barrier.

especially within coarse-grained LGM sand bodies.

In the interfluvial areas, where Pleistocene fluvial channel-belt sand bodies wedge out and are replaced by laterally continuous paleosols (interfluve sequence boundaries), groundwater flow paths are significantly different (Fig. 8). McArthur et al. (2008) suggested that Pleistocene aquifers are unpolluted because they are protected by the prominent Last Glacial Maximum paleosol from downward migration of arsenic and organic matter that drives As-pollution via reductive dissolution of As-bearing iron oxyhydroxides (Nickson et al., 1998; Smedley and Kinniburgh, 2002). Similarly, Hoque et al. (2012) and Ghosal et al. (2015) from the West Bengal documented that groundwaters polluted by As are essentially confined to Holocene channel-belt sand bodies, whereas low As values are observed below paleosols that protect the underlying aquifers against pollution. Chakraborty et al. (2022b) delineated a regional-scale hydrostratigraphic architecture where intervening aquitards in multi-layered, nearly confined aquifer subsystems, such as those examined in this work, appear to act as natural barriers to infiltration of surficial As or organic matter-rich water to the deeper aquifer zones.

In the Po Plain, another stiff paleosol horizon (paleosol YD in Fig. 2), younger than the LGM paleosol, directly underlies the Holocene organic-rich peaty muds (Figs. 7B and 8) and is likely to prevent the downward flow of groundwater into Pleistocene sand, protecting the aquifer from downward migrating arsenic and organic matter. In such a stratigraphic configuration, no remarkable arsenic-enriched groundwater seeping through the Holocene clay into the Pleistocene aquifer system is expected (Goodbred and Kuehl, 2000).

The high-resolution sequence-stratigraphic framework reconstructed for the Po Plain even reinforces McArthur's model, as (i) overconsolidated Pleistocene floodplain deposits in interfluvial areas represent poorly permeable (or possibly impermeable) units that hamper connectivity of Holocene and Pleistocene aquifers (Larue and Hovadik, 2006; Donselaar et al., 2017), and (ii) interfluvial areas host a set of closely-spaced paleosols (Amorosi et al., 2017b), instead of a single (LGM) paleosol, that are likely to represent multiple hydraulic barriers against the vertical migration of contaminants (Hoque et al., 2014) and

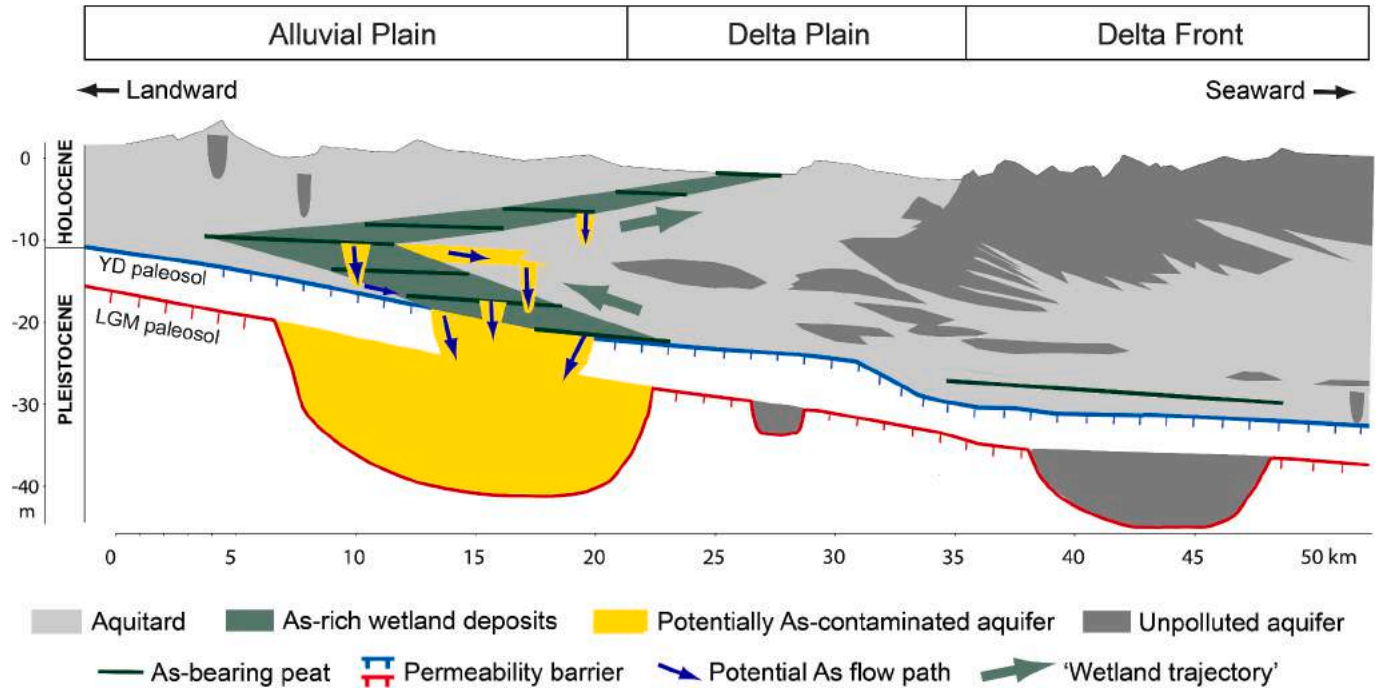

Fig. 8. Conceptual model for the accumulation and possible release of arsenic in shallow aquifer systems of modern coastal lowlands, based on the example from the Po Plain. Peat-rich deposits represent the major source of As to the groundwater system and their spatial distribution in the subsurface is expected to follow the trajectory of wetlands during the Holocene. Paleosol architecture is likely to exert a major control on flow paths: arsenic transport from the As-rich aquitard to contiguous aquifers occur primarily at the boundary between peat-bearing deposits and fluvial sand bodies.

that therefore may compartmentalize the aquifer system in terms of permeability (Fig. 8). The global eustatic and climatic control on paleosol formation (Bruno et al., 2020) suggests this picture can reasonably be extrapolated on a worldwide scale (McArthur et al., 2004).

Delineating precisely groundwater As-contaminated and As-safe areas, as well as predicting the proportion of the at-risk population that will be actually exposed to elevated levels of As, is a difficult task (Ravenscroft, 2007). In this study, we suggest that spatial patterns of arsenic concentration in the subsurface of modern coastal lowlands are not random. Using principles of sequence stratigraphy, we develop a set of predictive rules that rely on global controlling factors, and build a generalized model of As distribution beyond the regional scale (Figs. 2 and 8). Specifically, we can predict localized large As concentrations as a function of key stratigraphic features and delineate zones of elevated As-hazard in the Pleistocene/Holocene successions buried beneath modern alluvial/delta plains.

The lateral shift of wetland environments through time (here named the "wetland trajectory" – Fig. 8) under the combined effect of eustatic rise, local subsidence and sediment supply and the resulting Late Pleistocene-Holocene stratigraphy play a fundamental role in dictating natural As distribution in the subsurface. The early Holocene rise in sea level was accompanied by a landward shift of depositional environments, which in turn was followed by rapid delta progradation, starting at about 8000 cal yr BP (Stanley and Warne, 1994). The Holocene transgressive-regressive cycle resulted in a characteristic wedge-shaped facies architecture (Fig. 2) that has been widely reported in the literature (Curray and Moore, 1964; Oomkens, 1970; Frazier, 1974; Demarest and Kraft, 1987; Suter et al., 1987; Stanley and Warne, 1994).

Holocene peat-bearing deposits rich in arsenic are expected to accumulate landward of the marine transgression terminus (Syvitski et al., 2022) with distinctive wedge-shaped geometry (Fig. 8). They correlate distally to thin tongues of brackish (lagoon) clays and to thick, coastal sand and prodelta clay successions (Fig. 2), all characterized by low to negligible As contents (Fig. 4). Similarly, wetland deposits correlate at more proximal locations to As-poor alluvial plain facies, including lens-shaped fluvial bodies and overbank fines.

In general, we found a weak spatial relationship between surficial and subsurface distribution of arsenic: specifically, the surficial location of modern, organic-matter-rich (and As-rich) wetlands (e.g. delta plains) is not reflected in the subsurface by the spatial distribution of the thickest peat-bearing successions, which occur, instead, in a considerably more landward position, consistent with the Late Holocene coastal progradation (Fig. 8). According to our model, higher probabilities of elevated arsenic concentrations in groundwater (in conjunction with stratigraphic intervals where peat-bearing units are thickest) will be widespread beneath the (As-poor) active floodplain (Fig. 8).

The model shown in this paper is designed to reflect the spatial As variability across the shallow subsurface and to assess vulnerability of modern delta regions to elevated As-exposure. Large, tide-dominated deltas, being potentially particularly rich in wetlands as a result of the tidal excursion are likely to be much prone to arsenic accumulation than smaller, river- or wave-dominated deltas. Although the model may not entirely represent the stratigraphic variability of As due to local-scale heterogeneities, given the worldwide application of sequence-stratigraphic principles, well beyond the regional scale of individual delta systems, this model is expected to yield a high prediction accuracy. It also may enhance hydrostratigraphic models in highly urbanized and industrialized areas that suffer from sever groundwater As contamination (Chakraborty et al., 2022a, 2022b), allowing precise assessment of natural background levels versus anthropogenic contamination. Furthermore, this model can successfully help to identify areas with unrecognised arsenic pollution.

Establishing the extent to which organic matter represents a direct sink or source of arsenic in the peat-bearing successions of the Po Basin and assessing the (bio)geochemical processes by which arsenic is mobilized in the subsurface from solid matrices and released to the aquifer are largely beyond the scope of this study. Hydrogeological data and geochemical data on groundwater are not accounted for in the model presented here, which is based uniquely on stratigraphic, sedimentological and geochemical data from solid matrices and that, for this

reason, it cannot capture the complexities of groundwater flow paths. Further study and additional independent data on As concentrations in groundwater flowing through the different parts of the aquifer system are needed to validate and improve the predictive power of the model beyond the regional scale.

6. Conclusions

The concentration of arsenic of natural origin in Holocene peat-bearing deposits of the Po Plain is systematically surpassing the Italian threshold limit for contaminated soils. Through accurate assessment of As background values in 570 samples from nine types of solid matrices that reflect particular depositional environments and sediment grain size, we document that different lithofacies assemblages have distinctive background As levels, and build a general model of natural As distribution.

A high proportion of laterally continuous peat layers has the strongest influence on patterns of high arsenic concentrations within Quaternary estuarine/deltaic depositional systems and likely on As transfer to groundwater. Arsenic concentrations drop considerably in peat-free deposits, and negligible contents were found in conjunction with sand-dominated lithofacies. Arsenic distribution found in >2.5 m deep deposits, for which anthropogenic effects can be ruled out, compares with concentrations in near-surface sediments.

Naturally high arsenic concentrations in thick, alluvial/coastal plain successions that may host an abundance of As-bearing peat can spatially be predicted on the basis of sequence stratigraphic principles. In particular:

1. Thick and laterally extensive wetland deposits developed landward of the Holocene maximum marine ingression have been identified as the key source of As.
2. The "wetland trajectory", i.e. the path taken by landward-shifting and then seaward-migrating, peat-rich depositional environments during the Holocene, can be reconstructed across two-dimensional profiles and delineates the areas of potentially highest As concentration in the subsurface.
3. The superposition of thick and laterally continuous successions of Holocene peat-rich deposits formed in back-stepping estuarine environments (incised-valley fills) onto Pleistocene channel-belt sand bodies may account for As contamination of adjacent (Holocene) and underlying (Late Pleistocene) aquifer systems.
4. The volume of As-rich, estuarine Early-Middle Holocene deposits buried beneath modern coastal lowlands is significantly larger than the volume of near-surface (Late Holocene) As-rich deposits cropping out in recently abandoned meander belts, that are commonly considered the major source for As to the underlying aquifers.

Based on well-constrained depositional patterns of fluvio-deltaic facies architecture, which reflect a global control by late Quaternary sea-level fluctuations, we decipher the types of sediment contributing to higher arsenic concentration and determine portions of the aquifer system that have increased probability of elevated arsenic concentrations in groundwater. Subsurface stratigraphy and sedimentology, thus, can delineate areas with the highest groundwater contamination potential in coastal fringe settings.

Supplementary data to this article can be found online at https://doi.org/10.1016/j.scitotenv.2024.171571.

Funding

This work was supported by resources available at BiGeA, University of Bologna.

CRediT authorship contribution statement

Alessandro Amorosi: Writing – original draft, Supervision, Project administration, Methodology, Investigation, Funding acquisition, Formal analysis, Data curation, Conceptualization. **Irene Sammartino:** Writing – original draft, Methodology, Investigation, Formal analysis, Data curation, Conceptualization.

Declaration of competing interest

The authors declare that they have no known competing financial interests or personal relationships that could have appeared to influence the work reported in this paper.

Data availability

Data will be made available on request.

Acknowledgements

The authors give their sincere thanks to Corrado Piccinetti and Thomas Guercia for providing near-surface samples from the Adriatic offshore. Near-surface samples from Tuscan coastal swamps were kindly supplied by Elisabetta Bosi.

References

Acharyya, S.K., Shah, B.A., 2007. Arsenic-contaminated groundwater from parts of Damodar fan-delta and west of Bhagirathi River, West Bengal, India: influence of fluvial geomorphology and Quaternary morphostratigraphy. Environ. Geol. 52, 489–501.

Acharyya, S.K., Lahiri, S., Raymahashay, B.C., Bhowmik, A., 2000. Arsenic toxicity of groundwater in parts of the Bengal basin in India and Bangladesh: the role of Quaternary stratigraphy and Holocene sea-level fluctuation. Environ. Geol. 39, 1127–1137.

Amorosi, A., Sammartino, I., 2007. Influence of sediment provenance on background values of potentially toxic metals from near-surface sediments of Po coastal plain (Italy). Int. J. Earth Sci. 96, 389–396.

Amorosi, A., Centineo, M.C., Dinelli, E., Lucchini, F., Tateo, F., 2002. Geochemical and mineralogical variations as indicators of provenance changes in Late Quaternary deposits of SE Po Plain. Sediment. Geol. 151, 273–292.

Amorosi, A., Pavesi, M., Ricci, Lucchi M., Sarti, G., Piccin, A., 2008. Climatic signature of cyclic fluvial architecture from the Quaternary of the central Po Plain, Italy. Sediment. Geol. 209, 58–68.

Amorosi, A., Guermandi, M., Marchi, N., Sammartino, I., 2014. Fingerprinting sedimentary and soil units by their natural metal contents: a new approach to assess metal contamination. Sci. Total Environ. 500–501, 361–372.

Amorosi, A., Bruno, L., Campo, B., Rossi, V., Scarponi, D., Hong, W., Bohacs, K.M., Drexler, T.M., 2017a. Global sea-level control on local parasequence architecture from the Holocene record of the Po Plain, Italy. Mar. Pet. Geol. 87, 99–111.

Amorosi, A., Bruno, L., Cleveland, D.M., Morelli, A., Hong, W., 2017b. Paleosols and associated channel-belt sand bodies from a continuously subsiding late Quaternary system (Po Basin, Italy): new insights into continental sequence stratigraphy. Geol. Soc. Am. Bull. 129, 449–463.

Amorosi, A., Barbieri, G., Bruno, L., Campo, B., Drexler, T.M., Hong, W., Rossi, V., Sammartino, I., Scarponi, D., Vaiani, S.C., Bohacs, K.M., 2019. Three-fold nature of coastal progradation during the Holocene eustatic highstand, Po Plain, Italy—close correspondence of stratal character with distribution patterns. Sedimentology 66, 3029–3052.

Amorosi, A., Bruno, L., Campo, B., Costagli, B., Dinelli, E., Sammartino, I., Vaiani, S.C., 2020. Tracing clinothem geometry and sediment pathways in the prograding Holocene Po Delta system through integrated core stratigraphy. Basin Res. 32, 206–215.

Amorosi, A., Bruno, L., Cacciari, M., Campo, B., Rossi, V., 2021a. Tracing marine flooding surface equivalents across freshwater peats and other wetland deposits by integrated sedimentological and pollen data. Int. J. Coal Geol. 246 https://doi.org/10.1016/j.coal.2021.103830.

Amorosi, A., Bruno, L., Campo, B., Di Martino, A., Sammartino, I., 2021b. Patterns of geochemical variability across weakly developed paleosol profiles and their role as regional stratigraphic markers (Upper Pleistocene, Po Plain). Palaeogeogr. Palaeoclimatol. Palaeoecol. 574 https://doi.org/10.1016/j.palaeo.2021.110413.

Berg, M., Tran, H.C., Nguyen, T.C., Pham, H.V., Schertenleib, R., Giger, W., 2001. Arsenic contamination of groundwater and drinking water in Vietnam: a human health threat. Environ. Sci. Technol. 35, 2621–2626.

Berg, M., Stengel, C., Pham, T.K.T., Pham, H.V., Sampson, M.L., Leng, M., Samreth, S., Fredericks, D., 2007. Magnitude of arsenic pollution in the Mekong and Red River Deltas — Cambodia and Vietnam. Sci. Total Environ. 372, 413–425.

Berg, M., Pham, T.K.T., Stengel, C., Buschmann, J., Pham, V.H., Nguyen, D.V., Giger, W., Stüben, D., 2008. Hydrological and sedimentary controls leading to arsenic contamination of groundwater in the Hanoi area, Vietnam: the impact of iron-arsenic ratios, peat, river bank deposits and excessive groundwater abstraction. Chem. Geol. 249, 91–112.

Bhattacharya, P., Chatterjee, D., Jacks, G., 1997. Occurrence of arsenic-contaminated groundwater in alluvial aquifers from delta plains, Eastern India: options for safe drinking water supply. J. Water Resour. Dev. 13, 79–92.

Blanchard, M., Alfredsson, M., Brodholt, J., Wright, K., Catlow, R., 2007. Arsenic incorporation into FeS2 pyrite and its influence on dissolution: a DFT study. Geochim. Cosmochim. Acta 71, 624–630. https://doi.org/10.1016/j.gca.2006.09.021.

Bondesan, M., Favero, V., Viñals, M.J., 1995. New evidence on the evolution of the Po-Delta coastal plain during the Holocene. Quat. Int. 29–30, 105–110. https://doi.org/10.1016/1040-6182(95)00012-8.

Bosi, E., 2019. Tenori di fondo di arsenico in depositi olocenici della Pianura Padana (MSc Thesis). University of Bologna (88 pp.).

Bruno, L., Bohacs, K.M., Campo, B., Drexler, T.M., Rossi, V., Sammartino, I., Scarponi, D., Hong, W., Amorosi, A., 2017. Early Holocene transgressive palaeogeography in the Po coastal plain (Northern Italy). Sedimentology 64, 1792–1816.

Bruno, L., Campo, B., Di Martino, A., Hong, W., Amorosi, A., 2019. Peat layer accumulation and post-burial deformation during the mid-late Holocene in the Po coastal plain (Northern Italy). Basin Res. 31, 621–639.

Bruno, L., Marchi, M., Bertolini, I., Gottardi, G., Amorosi, A., 2020. Climate control on stacked paleosols in the Pleistocene of the Po Basin (northern Italy). J. Quat. Sci. 35, 559–571.

Campo, B., Amorosi, A., Bruno, L., 2016. Contrasting alluvial architecture of Late Pleistocene and Holocene deposits along a 120-km transect from the central Po Plain (northern Italy). Sediment. Geol. 341, 265–275.

Campo, B., Bruno, L., Amorosi, A., 2020. Basin-scale stratigraphic correlation of Late Pleistocene-Holocene (MIS 5e-MIS 1) strata across the rapidly subsiding Po Basin (northern Italy). Quat. Sci. Rev. 237 https://doi.org/10.1016/j.quascirev.2020.106300.

Carraro, A., Fabbri, P., Giaretta, A., Peruzzo, L., Tateo, F., Tellini, F., 2015. Effects of redox conditions on the control of arsenic mobility in shallow alluvial aquifers on the Venetian Plain (Italy). Sci. Total Environ. 532, 581–594.

Chakraborty, M., Sarkar, S., Mukherjee, A., Shamsudduha, M., Ahmed, K.M., Bhattacharya, A., Mitra, A., 2020. Modeling regional-scale groundwater arsenic hazard in the transboundary Ganges River Delta, India and Bangladesh: infusing physically-based model with machine learning. Sci. Total Environ. 748, 141107.

Chakraborty, M., Mukherjee, A., Ahmed, K.M., 2022a. Regional-scale hydrogeochemical evolution across the arsenic-enriched transboundary aquifers of the Ganges River Delta system, India and Bangladesh. Sci. Total Environ. 823, 153490.

Chakraborty, M., Mukherjee, A., Ahmed, K.M., Fryar, A.E., Bhattacharya, A., Zahid, A., Das, R., Chattopadhyay, S., 2022b. Influence of hydrostratigraphy on the distribution of groundwater arsenic in the transboundary Ganges River aquifer system, India and Bangladesh. Geol. Soc. Am. Bull. 134, 2680–2692.

Chatterjee, A., Das, D., Mandal, B.K., Roychowdhury, T., Samanta, G., Chakraborti, D., 1995. Arsenic in groundwater in six districts of West Bengal, India: the biggest calamity in the world, part I. Arsenic species in drinking water and urine of the affected people. Analyst 120, 643–650.

Chen, M., Zhang, Y., Ji, W., Chen, Q., Li, Y., Long, T., Wang, L., 2024. Source identification and exposure risk management for soil arsenic in urban reclamation areas with high background levels: a case study in a coastal reclamation site from the Pearl River Delta, China. J. Hazard. Mater. 465, 133294.

Correggiari, A., Cattaneo, A., Trincardi, F., 2005. The modern Po Delta system: lobe switching and asymmetric prodelta growth. Mar. Geol. 222–223, 49–74. https://doi.org/10.1016/j.margeo.2005.06.039.

Cubadda, F., Ciardullo, S., D'Amato, M., Raggi, A., Aureli, F., Carcea, M., 2010. Arsenic contamination of the environment–food chain: a survey on wheat as a test plant to investigate phytoavailable arsenic in Italian agricultural soils and as a source of inorganic arsenic in the diet. J. Agric. Food Chem. 58, 10176–10183.

Curray, J.R., Moore, D.G., 1964. Pleistocene deltaic progradation of continental terrace, Costa de Nayarit, Mexico. In: AAPG Memoir. Marine Geology of the Gulf of California, pp. 193–215.

Dang, T.T., Nguyen, N.T., Than, D.V., Nguyen, H.K., Kazmierczak, J., Pham, N.Q., 2020. The controlling of paleo-riverbed migration on arsenic mobilization in groundwater in the red River Delta, Vietnam. Vietnam J. Earth Sci. 42, 161–175.

Das, A., Mondal, S., 2021. Geomorphic controls on shallow groundwater arsenic contamination in Bengal basin, India. Environ. Sci. Pollut. Res. 28, 42177–42195.

de Meyer, C.M.C., Wahnfried, I., Rodriguez Rodriguez, J.M., Kipfer, R., García Avelino, P.A., Carpio Deza, E.A., Berg, M., 2023. Hotspots of geogenic arsenic and manganese contamination in groundwater of the floodplains in lowland Amazonia (South America). Sci. Total Environ. 860, 160407.

Demarest II, J.M., Kraft, J.C., 1987. Stratigraphic record of Quaternary sea levels: implications for more ancient strata. In: Nummedal, D., Piikey, O.H., Howard, J.D. (Eds.), Sea-level Fluctuations and Coastal Evolution, SEPM Special Publication, vol. 41, pp. 223–239.

Desbarats, A.J., Koenig, C.E.M., Pal, T., Mukherjee, P.K., Beckie, R.D., 2014. Groundwater flow dynamics and arsenic source characterization in an aquifer system of West Bengal, India. Water Resour. Res. 50 https://doi.org/10.1002/2013WR014034.

Di Giuseppe, D., Bianchini, G., Vittori Antisari, L., Martucci, A., Natali, C., Beccaluva, L., 2014. Geochemical characterization and biomonitoring of reclaimed soils in the Po River Delta (Northern Italy): implications for the agricultural activities. Environ. Monit. Assess. 186, 2925–2940.

Donselaar, M.E., Bhatt, A.G., Ghosh, A.K., 2017. On the relation between fluvio-deltaic flood basin geomorphology and the wide-spread occurrence of arsenic pollution in shallow aquifers. Sci. Total Environ. 574, 901–913.

Farooqui, A., Bajpai, U., 2003. Biogenic arsenopyrite in Holocene peat sediment, India. Ecotoxicol. Environ. Saf. 55, 157–161.

Filippini, M., Stumpp, C., Nijenhuis, I., Richnow, H.H., Gargini, A., 2015. Evaluation of aquifer recharge and vulnerability in an alluvial lowland using environmental tracers. J. Hydrol. 529, 1657–1668.

Filippini, M., Amorosi, A., Campo, B., Herrero-Martin, S., Nijenhuis, I., Parker, B.L., Gargini, A., 2016. Origin of VC-only plumes from naturally enhanced dechlorination in a peat-rich hydrogeologic setting. J. Contam. Hydrol. 192, 129–139.

Filippini, M., Zanotti, C., Bonomi, T., Sacchetti, V.G., Amorosi, A., Dinelli, E., Rotiroti, M., 2021. Deriving natural background levels of arsenic at the meso-scale using site-specific datasets: an unorthodox method. Water 13, 452.

Flint, S.S., Aitken, J., Hampson, G., 1995. Application of sequence stratigraphy to coal-bearing coastal plain successions: implications for the UK Coal Measures. In: Whateley, M.K.G., Spears, D.A. (Eds.), European Coal Geology: Geol. Soc., London, Spec. Publ, vol. 82, pp. 1–16.

Franzini, M., Leoni, L., Saitta, M., 1972. A simple method to evaluate the matrix effects in X-ray fluorescence analysis. X-Ray Spectrom. 1, 151–154.

Frazier, D.E., 1974. Depositional-episodes: their relationship to the Quaternary stratigraphic framework in the northwestern portion of the Gulf Basin. In: Bureau of Economic Geology, The University of Texas at Austin, Geological Circular, vol. 74, pp. 1–28.

Ghosal, U., Sikdar, P.K., McArthur, J.M., 2015. Palaeosol control of arsenic pollution: the Bengal Basin in West Bengal, India. Ground Water 53, 588–599.

Ghosh, D., Donselaar, M.E., 2023. Predictive geospatial model for arsenic accumulation in Holocene aquifers based on interactions of oxbow-lake biogeochemistry and alluvial geomorphology. Sci. Total Environ. 856, 158952.

Ghosh, D., Kumar, S., Donselaar, M.E., Corroto, C., Ghosh, A.K., 2021. Organic carbon transport model of abandoned river channels - a motif for floodplain geomorphology influencing biogeochemical swaying of arsenic. Sci. Total Environ. 762, 144400 https://doi.org/10.1016/j.scitotenv.2020.144400.

González, Z.I., Krachler, M., Cheburkin, A.K., Shotyk, W., 2006. Spatial distribution of natural enrichments of arsenic, selenium, and uranium in a mineratrophic peatland, Gola di Lago, Canton Ticino, Switzerland. Environ. Sci. Technol. 40, 6568–6574.

Goodbred, S.L., Kuehl, S.A., 2000. The significance of large sediment supply, active tectonism, and eustasy of margin sequence development: Late Quaternary stratigraphy and evolution of the Ganges–Brahmaputra delta. Sediment. Geol. 133, 227–248.

Goodbred, S.L., Paolo, P.M., Ullah, M.S., Pate, R.D., Khan, S.R., Kuehl, S.A., Rahaman, W., 2014. Piecing together the Ganges–Brahmaputra–Meghna River delta: use of sediment provenance to reconstruct the history and interaction of multiple fluvial systems during Holocene delta evolution. Geol. Soc. Am. Bull. 126, 1495–1510.

Herath, I., Vithanage, M., Bundschuh, J., Prakash Maity, J., Bhattacharya, P., 2016. Natural arsenic in global groundwaters: distribution and geochemical triggers for mobilization. Curr. Pollut. Rep. 2, 68–89.

Hoque, M.A., McArthur, J.M., Sikdar, P.K., 2012. The palaeosol model of arsenic pollution of groundwater tested along a 32 km traverse across West Bengal, India. Sci. Total Environ. 431, 157–165.

Hoque, M.A., McArthur, J.M., Sikdar, P.K., 2014. Sources of low-arsenic groundwater in the Bengal Basin: investigating the influence of the last glacial maximum palaeosol using a 115-km traverse across Bangladesh. Hydrogeol. J. 22, 1535–1547.

Huyen, D.T., Tabelin, C.B., Thuan, H.M., Dang, D.H., Truong, P.T., Vongphuthone, B., Kobayashi, M., Igarashi, T., 2019. Geological and geochemical characterizations of sediments in six borehole cores from the arsenic-contaminated aquifer of the Mekong Delta, Vietnam. Data Brief 25, 104230.

Jerrett, R.M., Flint, S.S., Davies, R.C., Hodgson, D.M., 2011. Sequence stratigraphic interpretation of a Pennsylvanian (Upper Carboniferous) coal from the central Appalachian Basin, USA. Sedimentology 58, 1180–1207.

Kabata-Pendias, A., Mukherjee, A.B., 2007. Trace Elements From Soil to Human. Springer-Verlag, Berlin, p. 550.

Kazmierczak, J., Postma, D., Dang, T., Van Hoang, H., Larsen, F., Hass, A.E., Hoffmann, A.H., Fensholt, R., Pham, N.Q., Jakobsen, R., 2022. Groundwater arsenic content related to the sedimentology and stratigraphy of the Red River delta, Vietnam. Sci. Total Environ. 814.

Kumar, S., Ghosh, D., Donselaar, M.E., Burgers, F., Ghosh, A.K., 2021. Clay-plug sediment as the locus of arsenic pollution in Holocene alluvial-plain aquifers. Catena 202, 105255. https://doi.org/10.1016/j.catena.2021.105255.

Langner, P., Mikutta, C., Kretzschmar, R., 2012. Arsenic sequestration by organic sulphur in peat. Nat. Geosci. 5, 66–73.

Larue, D.K., Hovadik, J., 2006. Connectivity of channelized reservoirs: a modeling approach. Pet. Geosci. 12, 291–308.

Legislative Decree 152, 2006. Decreto Legislativo n. 152 del 3 aprile 2006 sulle norme in materia ambientale (Legislative Decree on Environmental Regulations). Available online: https://www.isprambiente.gov.it/it/garante_aia_ilva/normativa/normativaambientale/Dlgs_152_06_TestoUnicoAmbientale.pdf.

Leoni, L., Saitta, M., 1976. Determination of yttrium and niobium on standard silicate rocks by X-ray fluorescence analyses. X-Ray Spectrom. 5, 29–30.

Leoni, L., Menichini, M., Saitta, M., 1982. Determination of S, Cl and F in silicate rocks by X-Ray fluorescence analyses. X-Ray Spectrom. 11, 156–158.

Marchi, N., Ungaro, F., 2019. Carta del Fondo naturale-antropico della Pianura emiliano-romagnola, scala 1: 250.000 - As, Cd, Cr, Cu, Ni, Pb, Sn, V, Zn, Servizio Geologico Sismico e dei Suoli - Regione Emilia-Romagna. https://datacatalog.regione.emilia-romagna.it/catalogCTA/dataset/carta-del-fondonaturale-antropico.

McArthur, J.M., Banerjee, D.M., Hudson-Edwards, K.A., Mishra, R., Purohit, R., Ravenscroft, P., Cronin, A., Howarth, R.J., Chatterjee, A., Talukder, T., Lowry, D., Houghton, S., Chadha, D.K., 2004. Natural organic matter in sedimentary basins and its relation to arsenic in anoxic groundwater: the example of West Bengal and its worldwide implications. Appl. Geochem. 19, 1255–1293.

McArthur, J.M., Ravenscroft, P., Banerjee, D.M., Milsom, J., Hudson-Edwards, K.A., Sengupta, S., Bristow, C., Sarkar, A., Tonkin, S., Purohit, R., 2008. How paleosols influence groundwater flow and arsenic pollution: a model from the Bengal Basin and its worldwide implication. Water Resour. Res. 44, W11411 https://doi.org/10.1029/2007WR006552.

McArthur, J.M., Nath, B., Banerjee, D.M., Purohit, R., Grassineau, N., 2011. Palaeosol control on groundwater flow and pollutant distribution: the example of arsenic. Environ. Sci. Technol. 45, 1376–1383.

Mikutta, C., Rothwell, J.J., 2016. Peat bogs as hotspots for organoarsenical formation and persistence. Environ. Sci. Technol. 50, 4314–4323.

Molinari, A., Guadagnini, L., Marcaccio, M., Guadagnini, A., 2015. Arsenic fractioning in natural solid matrices sampled in a deep groundwater body. Geoderma 247–248, 88–96.

Mukherjee, A., Fryar, A.E., Scanlon, B.R., Bhattacharya, P., Bhattacharya, A., 2011. Elevated arsenic in deeper groundwater of the western Bengal basin, India: extent and controls from regional to local scale. Appl. Geochem. 26, 600–613.

Nath, B., Berner, Z., Chatterjee, D., Mallik, S.B., Stuben, D., 2008. Mobility of arsenic in West Bengal aquifers conducting low and high groundwater arsenic. Part II: comparative geochemical profile and leaching study. Appl. Geochem. 23, 996–1011.

Nickson, R., McArthur, J., Burgess, W., Ahmed, K.M., Ravenscroft, P., Rahmanñ, M., 1998. Arsenic poisoning of Bangladesh groundwater. Nature 395, 338. https://doi.org/10.1038/26387.

Oomkens, E., 1970. Depositional sequences and sand distribution in the postglacial Rhone delta complex. In: Morgan, J.P. (Ed.), Deltaic Sedimentation, Modern and Ancient, SEPM Special Publication, vol. 15, pp. 198–212.

Papacostas, N.C., Bostick, B.C., Quicksall, A.N., Landis, J.D., Sampson, M., 2008. Geomorphic controls on groundwater arsenic distribution in the Mekong River Delta, Cambodia. Geology 36, 891–894.

Parks, G.A., 1990. Surface energy and adsorption at mineral-water interfaces: an introduction. In: Hochella Jr., M.F., White, A.F. (Eds.), Mineral-Water Interface Geochemistry. Mineralogical Society of America, Washington, D.C, pp. 133–175.

Paszkowski, A., Goodbred Jr., S., Borgomeo, E., Shah Alam Khan, M., Hall, J.W., 2021. Geomorphic change in the Ganges–Brahmaputra–Meghna delta. Nat. Rev. https://doi.org/10.1038/s43017-021-00213-4.

Polizzotto, M.L., Kocar, B.D., Benner, S.G., Sampson, M., Fendorf, S., 2008. Near-surface wetland sediments as a source of arsenic release to ground water in Asia. Nature 454, 505–509.

Polya, D.A., Gault, A.G., Diebe, N., Feldman, P., Rosenboom, J.W., Gilligan, E., Fredericks, D., Milton, A.H., Sampson, M., Rowland, H.A.L., Lythgoe, P.R., Jones, J. C., Middleton, C., Cooke, D.A., 2005. Arsenic hazard in shallow Cambodian groundwaters. Mineral. Mag. 69, 807–823.

Postma, D., Larsen, F., Thai, N.T., Pham, T.K.T., Jakobsen, R., Nhan, P.Q., Long, T.V., Viet, P.H., Murray, A.S., 2012. Groundwater arsenic concentrations in Vietnam controlled by sediment age. Nat. Geosci. 5, 656–661.

Postma, D., Pham, T.K.T., Sø, H.U., Hoang, V.H., Vi, M.L., Nguyen, T.T., Larsen, F., Pham, H.V., Jakobsen, R., 2016. A model for the evolution in water chemistry of an arsenic contaminated aquifer over the last 6000 years, Red River floodplain, Vietnam. Geochim. Cosmochim. Acta 195, 277–292.

Ravenscroft, P., 2007. Predicting the Global Extent of Arsenic Pollution of Groundwater and Its Potential Impact on Human Health. UNICEF, New York, pp. 1–27.

Ravenscroft, P., Brammer, H., Richards, K., 2009. Arsenic Pollution: A Global Synthesis. Wiley-Blackwell, Chichester. https://doi.org/10.1002/9781444308785.

Rotiroti, M., McArthur, J.M., Fumagalli, L., Stefania, G.A., Sacchi, E., Bonomi, T., 2017. Pollutant sources in an arsenic-affected multilayer aquifer in the Po Plain of Italy: implications for drinking-water supply. Sci. Total Environ. 578, 502–512.

Rotiroti, M., Bonomi, T., Sacchi, E., McArthur, J.M., Jakobsen, R., Sciarra, A., Etiope, G., Zanotti, C., Nava, V., Fumagalli, L., Leoni, B., 2021. Overlapping redox zones control arsenic pollution in Pleistocene multi-layer aquifers, the Po Plain (Italy). Sci. Total Environ. 758, 143646.

Sarti, S., Sammartino, I., Amorosi, A., 2020. Geochemical anomalies of potentially hazardous elements reflect catchment geology: an example from the Tyrrhenian coast of Italy. Sci. Total Environ. 714 https://doi.org/10.1016/j.scitotenv.2020.136870.

Smedley, P.L., Kinniburgh, D.G., 2002. A review of the source, behaviour and distribution of arsenic in natural waters. Appl. Geochem. 17, 517–568.

Stahl, M.O., Harvey, C.F., van Geen, A., Sun, J., Trang, P.T.K., Lan, V.M., Phuong, T.M., Viet, P.H., Bostick, B.C., 2016. River bank geomorphology controls groundwater arsenic concentrations in aquifers adjacent to the Red River, Hanoi Vietnam. Water Resour. Res. 52, 6321–6334.

Stanley, D.J., Warne, A.G., 1994. Worldwide initiation of Holocene marine deltas by deceleration of sea-level rise. Science 265, 228–231.

Stefani, M., Vincenzi, S., 2005. The interplay of eustasy, climate and human activity in the late Quaternary depositional evolution and sedimentary architecture of the Po Delta system. Mar. Geol. 222–223, 19–48. https://doi.org/10.1016/j.margeo.2005.06.029.

Stuckey, J.W., Schaefer, M.V., Kocar, B.D., Dittmar, J., Lezama Pacheco, J., Benner, S.G., Fendorf, S., 2015. Peat formation concentrates arsenic within sediment deposits of the Mekong Delta. Geochim. Cosmochim. Acta 149, 190–205.

Suter, R.J., Berryhill Jr., H.L., Penland, S., 1987. Late Quaternary sea-level fluctuations and depositional sequences, southwest Louisiana continental shelf. In: Nummedal, D., Pilkey, O.H., Howard, J.D. (Eds.), Sea-level Fluctuation and Coastal Evolution, SEPM Special Publication, vol. 41, pp. 199–219.

Syvitski, J., Anthony, E., Saito, Y., Zainescu, F., Day, J., Bhattacharya, J.P., Giosan, L., 2022. Large deltas, small deltas: toward a more rigorous understanding of coastal marine deltas. Glob. Planet. Chang. 218, 103958.

Tarvainen, T., Albanese, S., Birke, M., Ponavic, M., 2013. Arsenic in agricultural and grazing land soils of Europe. Appl. Geochem. 28, 2–10.

Ungaro, F., Ragazzi, F., Cappellin, R., Giandon, P., 2008. Arsenic concentration in the soils of the Brenta Plain (Northern Italy): mapping the probability of exceeding contamination thresholds. J. Geochem. Explor. 96, 117–131.

van Geen, A., Zheng, Y., Versteeg, R., Stute, M., Horneman, A., Dhar, R., Steckler, M., Gelman, A., Small, C., Ahsan, H., Graziano, J.H., Hussain, I., Ahmed, K.M., 2003. Spatial variability of arsenic in 6000 tube wells in a 25 km^2 area of Bangladesh. Water Resour. Res. 39 https://doi.org/10.1029/2002WR001617.

van Geen, A., Bostick, B.C., Pham, T.K.T., Vi, M.L., Nguyen-Ngoc, M., Phu, D.M., Pham, H.V., Radloff, K., Aziz, Z., Mey, J.L., Stahl, M.O., Harvey, C.F., Oates, P., Weinman, B., Stengel, C., Frei, F., Kipfer, R., Berg, M., 2013. Retardation of arsenic transport through a pleistocene aquifer. Nature 501, 204–207. https://doi.org/10.1038/nature12444.

Veggiani, A., 1974. Le variazioni idrografiche del basso corso del fiume Po negli ultimi 3000 anni. Padusa 1–2, 39–60.

Wang, Y., Le Pape, P., Morin, G., Asta, M.P., King, G., Bártová, B., Suvorova, E., Frutschi, M., Ikogou, M., Pham, V.H.C., Vo, P.L., Herman, F., Charlet, L., Bernier-Latmani, R., 2018. Arsenic speciation in Mekong Delta sediments depends on their depositional environment. Environ. Sci. Technol. 52, 3431–3439.

Wang, Y., Pi, K., Fendorf, S., Deng, Y., Xie, X., 2019. Sedimentogenesis and hydrobiogeochemistry of high arsenic Late Pleistocene-Holocene aquifer systems. Earth Sci. Rev. 189, 79–98.

Weinman, B., Goodbred, S.L., Zheng, Y., Aziz, Z., Steckler, M., van Geen, A., Singhvi, A. K., Nagar, Y.C., 2008. Contributions of floodplain stratigraphy and evolution to the spatial patterns of groundwater arsenic in Araihazar, Bangladesh. Geol. Soc. Am. Bull. 120, 1567–1580.

Winkel, L.H.E., Pham, T.K.T., Vi, M.L., Stengel, C., Amini, M., Nguyen, T.H., Pham, H.V., Berg, M., 2011. Arsenic pollution of groundwater in Vietnam exacerbated by deep aquifer exploitation for more than a century. Proc. Natl. Acad. Sci. USA 108, 1246–1251.

Xu, N., Zhang, F., Xu, N., Li, L., Liu, L., 2023. Chemical and mineralogical variability of sediment in a Quaternary aquifer from Huaihe River Basin, China: implications for groundwater arsenic source and its mobilization. Sci. Total Environ. 865, 160864.

Yamazaki, C., Ishiga, H., Ahmed, F., Itoh, K., Suyama, K., Yamamoto, H., 2003. Vertical distribution of arsenic in ganges delta sediments in Deuli Village, Bangladesh. Soil Sci. Plant Nutr. 49, 567–574.

Zanotti, C., Caschetto, M., Bonomi, T., Parini, M., Cipriano, G., Fumagalli, L., Rotiroti, M., 2022. Linking local natural background levels in groundwater to their generating hydrogeochemical processes in Quaternary alluvial aquifers. Sci. Total Environ. 805, 150259.

Zonta, R., Cassin, D., Pini, R., Dominik, J., 2019. Assessment of heavy metal and As contamination in the surface sediments of Po delta lagoons (Italy). Estuar. Coast. Shelf Sci. 225, 106235.

Zuzolo, D., Cicchella, D., Demetriades, A., Birke, M., Albanese, S., Dinelli, E., Lima, A., Valera, P., De Vivo, B., 2020. Arsenic: geochemical distribution and age-related health risk in Italy. Environ. Res. 182, 109076.